Tampere University

Mohammad Taqi Tahmid

AVAILABLE 5G NR REFERENCE SIGNALS AND THEIR POTENTIAL FOR 5G NR POSITIONING

Master of Science Thesis
Faculty of Information Technology and Communication Sciences
November 2020

ABSTRACT

Taqi Tahmid: Available 5G NR Reference Signals and their Potential for 5G NR Positioning
Master of Science Thesis
Tampere University
Wireless Communication and RF Systems
Supervisors: University lecturer Jukka Talvitie and Doctoral researcher Mike Koivisto
November 2020

The fifth-generation (5G) cellular network technology standard is bringing massive improvements and many new innovative features in cellular communications and 5G new radio (NR) based positioning is among them. Traditional Global Navigation Satellite System (GNSS) based positioning provides adequate positioning accuracy in outdoor environments but struggles where direct Line of Sight (LOS) communication with the satellites is not possible especially in indoor environments. This new 5G NR based positioning is a promising approach to improve the positioning accuracy in both indoor and outdoor environments. In order to implement this new positioning technology, either a dedicated reference signal for positioning could be introduced or existing reference signals could be utilized to carry out additional positioning responsibility. In our work, we have explored the possibility of availing these existing reference signals for positioning. At first, we have reviewed different wireless communication based positioning systems. Next, we have studied the time and frequency domain resource allocation of uplink and downlink reference signals. After that, we have analyzed and compared the performance, and geometrical influence of the reference signals for Time of Arrival (TOA) and Angle of Arrival (AOA) based positioning technique and demonstrated that these existing reference signals might be capable of positioning responsibility without introducing a dedicated positioning reference signal.

Keywords: 5G, NR, 3GPP, positioning, 5G NR positioning, 5G reference signal, TOA, AOA

PREFACE

Firstly, I would like to thank the admission committee of Tampere University for giving me the opportunity to study in one of the most prestigious universities in Finland. While working on the thesis, I received utmost help from the faculty members and my class-mates. Their guidelines and motivation inspired me to complete the work in time.

Next, I would like to express my deepest gratitude towards my thesis supervisors Jukka Talvitie and Mike Koivisto for their continuous support and day-to-day feedback on the thesis writing which helped me a lot in shaping up the thesis.

Finally, I would like to thank my parents (Sabbir Hossain and Nasrin Sultana) for their love and support from overseas.

Tampere, 29 November 2020

Mohammad Taqi Tahmid

CONTENTS

LIST OF FIGURES

LIST OF TABLES

LIST OF SYMBOLS AND ABBREVIATIONS

3GPP	3rd Generation Partnership Project
4G	Fourth Generation
5G	Fifth Generation
AOA	Angle of Arrival
AR	Augmented Reality
BLE	Bluetooth Low Energy
BS	Base Station
BW	Bandwidth
CORESET	Control Resource Set
CRLB	Cramér–Rao Lower Bound
CSI-RS	Channel State Information Reference Signal
DCI	Downlink Control Information
DMRS	Demodulation Reference Signal
EMBB	Enhanced/Extreme/Evolved Mobile Broadband
FR1	Frequency Range 1
FR2	Frequency Range 2
GNSS	Global Navigation Satellite Systems
GPS	Global Positioning System
IMU	Inertial Measurement Unit
IoT	Internet of Things
IRNSS	Indian Regional Navigational Satellite System
LAI	Location Area Identity
LOS	Line of Sight
LPWA	Low power Wide Area
LTE	Long Term Evolution
MMTC	Massive Machine Type Communication
MT	Mobile Terminal
NLOS	Non Line of Sight
NR	New Radio
OFDM	Orthogonal Frequency Division Multiplexing
PBCH	Physical Broadcast Channel
PDP	Power Delay Profile
PDSCH	Physical Downlink Shared Channel
PEB	Position Error Bound
PSS	Primary Synchronization Signal
PTRS	Phase Tracking Reference Signal
PUSCH	Physical Uplink Shared Channel
QoS	Quality of Service
QZSS	Quasi Zenith Satellite System
RAN	Radio Access Network
RAT	Radio Access Technology
RFID	Radio Frequency Identification
RMSE	Root Mean Square Error
RSS	Received Signal Strength
RTTOA	Round-Trip Time of Arrival
SNR	Signal to Noise Ratio
SRS	Sounding Reference Signal
SSS	Secondary Synchronization Signal
TBS	Terrestrial Beacon Systems
TDOA	Time Difference of Arrival
TOA	Time of Arrival
TTFF	Time to First Fix

TWR	Two Way Ranging
UAV	Unmanned Aerial Vehicle
URLLC	Ultra Reliable and Low Latency Communication
UWB	Ultra Wide Band
VR	Virtual Reality
V2X	Vehicle-to-Everything
WIFI	Wireless Fidelity
WPAN	Wireless Personal Area Network
XR	Anything Reality

1. INTRODUCTION

Fifth Generation (5G) is the up and coming mobile network standard that will revolutionize the mobile telecommunication industry with not only enhanced mobile broadband services but also with the introduction of numerous new features and solutions. 5G will expand the mobile network to incorporate machines, devices, vehicles, and objects and enable industries to use its services for improved performance, efficiency, and cost. Artificial Intelligence, cloud, and robotics will redefine a broad range of social and industrial sectors which will be driven by 5G. Implementation of 5G will also empower the full potential of the Internet of Things (IoT) which in terms aims to create an interconnected world where every device is connected. 5G will utilize new frequency bands termed as new radio (NR) frequency range 2 (FR2) as well as existing bands frequency range 1 (FR1) for mobile communication as shown in Figure 1 to meet the requirements of its diverse sets of services and use cases.

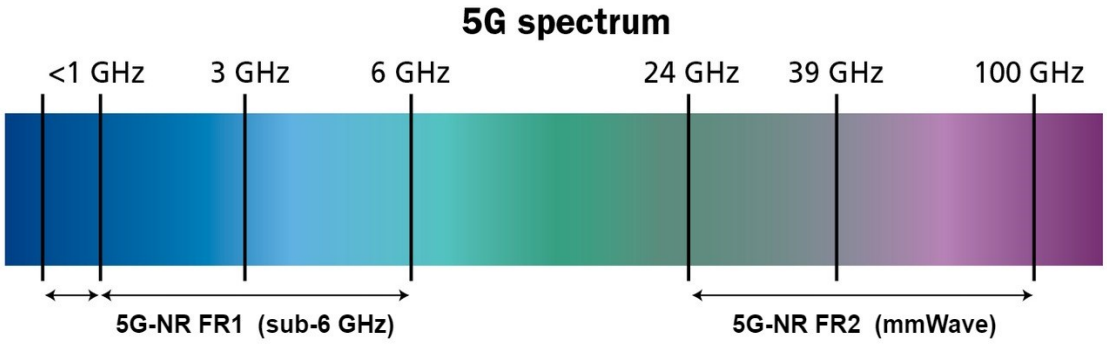

Figure 1 *5G supported bands in both licensed and unlicensed spectrum*

Over the past years, positioning and navigation usage has become extensive with the improvements of mobile network which enables widespread usage of mobile broadband service. Due to the extensive availability of the mobile broadband and Global Positioning System (GPS) receivers baked into the mobile devices, Global Navigation Satellite Systems (GNSS) have been the typical source of accurate positioning for end devices. However, the positioning accuracy for different GNSS services such as GPS is around 2-5 meters [1] and in indoors and tunnels, the services are degraded even more as GPS satellites mainly communicate with the device via Line of Sight (LOS) communication.

The reason for this modification is that the GPS is mainly based on one-way communication and it still transmits signals towards the Earth even though the devices are in non-line of sight (NLOS). The introduction of 5G will enable 5G based standalone positioning [2] as well as a combination of GNSS and cell-based positioning to address these shortcomings and provide reliable, efficient, and accurate position estimates for both indoor and outdoor scenarios to meet the growing demand for very high accurate positioning use cases, such as autonomous vehicle navigation, Industrial IoT applications, Unmanned Areal Vehicle (UAV) missions, and operations, for instance. 5G NR based positioning aims to achieve below 1 m positioning accuracy for both indoor and outdoor scenarios and even less than 30 cm accuracy for automotive applications such as autonomous driving, collision avoidance, platooning, etc [3]. 5G will introduce large antenna arrays and bandwidths along with ultra-dense 5G base station deployments which will allow more accurate time of arrival (TOA) and angle of arrival (AOA) estimation [4] and enable more accurate positioning performance.

In order to reach such positioning performance with 5G NR, one potential solution could be to employ existing reference signals for positioning purposes. The reference signals are known signals which are utilized in important physical layer tasks such as channel estimation, channel equalization, provide required information about the communication channel, etc. According to the third generation partnership project (3GPP) TS 38.211 [5], there are three reference signals in uplink and five reference signals in the downlink for 5G. The uplink reference signals are demodulation reference Signal (DMRS), phase-tracking reference signal (PTRS), and sounding reference signal (SRS); and the downlink reference signals are DMRS, PTRS, channel- state information reference signal (CSI-RS), primary synchronization signal (PSS), and secondary synchronization signal (SSS). Each of the reference signals is intended for a different purpose and transmitted in diverse ways. The main difference between Fourth Generation (4G) Long Term Evaluation (LTE) and 5G reference signals is that unlike transmitting a subset of reference signals in an always-on manner in LTE, reference signals will be transmitted only when necessary in 5G. 5G NR has introduced different downlink reference signals to replace the LTE cell-specific reference signal for coherent demodulation, channel quality estimation and general time-frequency tracking [6].

In this thesis, the 5G reference signals and their feasibility to be used for 5G NR based positioning is broadly discussed and evaluated. There are two main characteristics of the reference signals that have been taken into account to evaluate their ability to convey real-time positioning data for very high accuracy positioning.

The first aspect is time domain resource allocation, and the second aspect is frequency domain resource allocation to each reference signals both in uplink and downlink and how often they are repeated during transmission. Despite 5G allows quite a lot of configurability of these reference signals in terms of resource allocation to tackle different transmission scenarios, here the maximum allowable time and frequency domain resources have been considered for these reference signals to evaluate positioning performance.

The thesis is organized as follows. In section 2, a detailed description of 5G NR, its features and use cases, its advantages over earlier mobile network standards have been discussed. A concise explanation of available positioning solutions, their working principle, advantages, and disadvantages have also been discussed in this section. In section 3, 5G uplink and downlink reference signals, their functions, and resource allocations have been analyzed. The TOA and AOA based positioning performance and geometrical influence measurement methodologies have been discussed in section 4. The performance evaluation and geometrical influence of 5G reference signals in terms of TOA and AOA based positioning have been performed in section 5. The conclusion of this thesis has been drawn in the final section.

2. BACKGROUND STUDIES

In this chapter, background studies related to the thesis topic have been presented. This chapter consists of five sections. They are (i) 5G NR, (ii) Positioning methods, (iii) Ground based positioning system, (iv) Satellite based positioning system, (v) Wireless communication based positioning system.

2.1 5G NR

5G is the next generation of mobile network technology that aims to supplement or replace all previous network technologies. Unlike 4G, Third Generation (3G), and any other network technologies, 5G is unique. It aims to take a much larger role and introduce numerous new features and services as well as improve the existing technologies. In order to realize 5G visions, a more capable, robust, and united radio access technology (RAT) will be required to meet the connectivity demands in days to come. The 5G NR standards are developed by 3GPP to meet the diverse 5G requirements, services, and features, and to enable remarkably higher performance more efficiently and at a much lower cost. 5G NR plans to utilize licensed, unlicensed, and shared spectrum across all bands from low to medium to high bands known as millimeter wave bands. The low bands below 1 GHz provide a relatively long range and will be preferable for mobile broadband and massive IoT. The mid bands between 1 GHz and 6 GHz provide wider bandwidth and will be suitable for enhanced mobile broadband and mission-critical applications. And the high bands above 24 GHz (mmWave) will make available an extensive amount of bandwidth for extreme data rates and capacity which has not been realized before in mobile communications [7].

The upcoming 5G use cases can be categorized into three major services as can be seen from Figure 2:

- Enhanced/Extreme/Evolved Mobile Broadband (EMBB)
- Massive Machine Type Communication (MMTC) or massive IoT
- Ultra Reliable and Low Latency Communication (URLLC)

EMBB will provide high throughput and always available mobile broadband access in specific locations, such as crowded areas, high-speed public transport systems, across a wide coverage area, etc. It will enhance the current mobile broadband capability of 4G technology with higher availability and greater Quality of Service (QoS) across all

scenarios. The EMBB aims to enable higher capacity, enhanced connectivity, and higher user mobility in 5G. The higher capacity will ensure the availability of broadband service in both indoors and outdoors and densely populated areas, such as city centers, office buildings, downtowns. The enhanced connectivity will allow broadband service to be available more broadly to cater to consistent user experience. Besides, higher user mobility will enable mobile broadband services in moving vehicles including high-speed trains, cars, buses, planes, to name a few [8].

Massive Machine Type Communication or massive IoT will offer Low Power Wide Area (LPWA) connections to devices that require low data rate, low cost, and long battery life. This service will enable the interconnection of millions of devices to create a truly connected world while ensuring cost efficiency and robust security. There is huge market potential in massive IoT applications in the coming years due to the increasing interest toward wearables (health tracking), asset tracking (logistics), environmental monitoring, smart city, smart home, smart manufacturing (monitoring, tracking, digital twins) smart metering, among others [9].

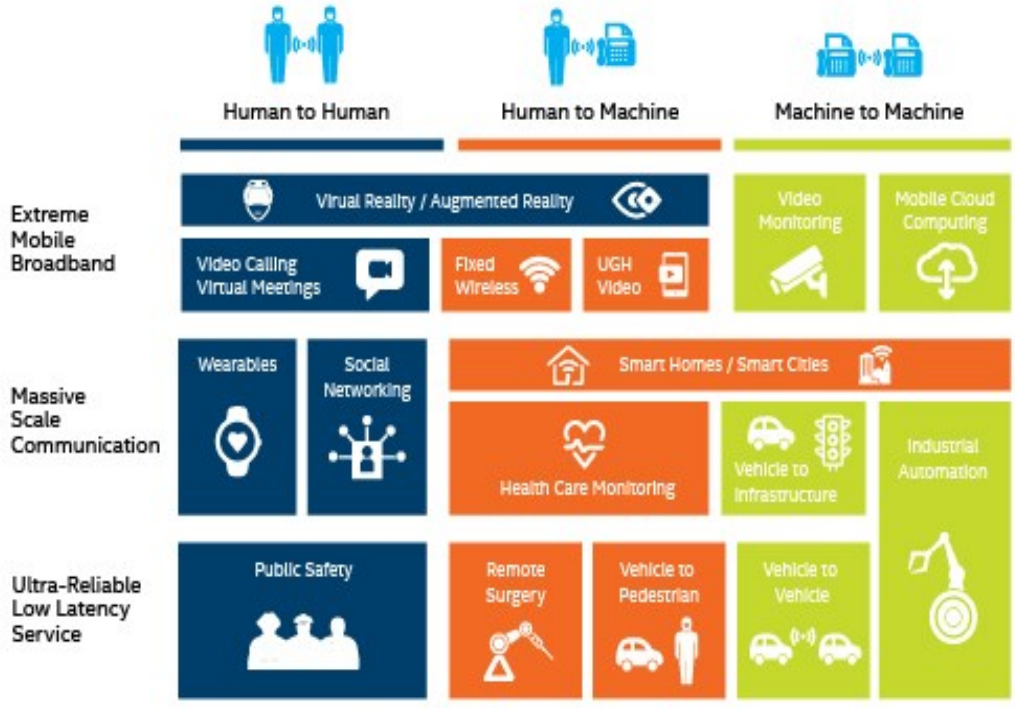

Figure 2. *5G use cases* [10]

URLLC is one of the most significant additions of service provided by the 5G NR. Various new technologies and services that require ultra reliable and very low latency network connection will depend upon the implementation of URLLC service. URLLC will be essential for autonomous vehicles, real-time control and automation of industrial

processes, emergency communication in disaster and public safety, vehicle to vehicle communication, Virtual Reality (VR), Augmented Reality (AR), Tactile Internet, and so on. URLLC will rapidly increase the efficiency, safety, and overcome the limitations of long-distance communication to drive the manufacturing and other industries into a new era [11].

The standardization of 5G NR started with the 3GPP release 15 in 2018. Release 16 and 17 have included a further enhancement for the 5G NR to be more applicable and available in future industrial and public sectors. The release 16 enhancements include multiple inputs and multiple outputs (MIMO) and beamforming enhancements, dynamic spectrum sharing, dual connectivity and carrier aggregation, mobile terminal power saving among others. The release 16 has also included new verticals and deployment scenarios such as integrated access and backhaul, NR in unlicensed spectrum, a feature related to Industrial IoT and URLLC, intelligent transportation system, vehicle-to-anything (V2X) communications [12]. The release 17 will further enhance the release 15 and 16 features and will introduce new scenarios for the three new use cases: URLLC, EMBB, and mMTC. The enhancement for the URLLC includes improved support for factory automation, high accuracy and low latency positioning, sidelink, Radio Access Network (RAN) slicing for instance. The enhancement for the eMBB contains improved duplexing of access and backhaul links, routing enhancements, cross-carrier scheduling enhancement, more efficient activation and deactivation mechanism of secondary cells to name a few. The enhancement for the MMTC includes reduced overhead from connection establishment. In addition to that release 17 will also include new features for the three use cases. The new EMBB feature includes supporting NR from 52.6 GHz to 71 GHz, multicast and broadcast services, support for non-terrestrial networks for instance. The new URLLC and eMTC feature include anything reality (XR) evaluations, support for reduced capability NR devices among others [13].

The demand for network based positioning is increasing rapidly due to the newly proposed use cases, such as vehicular connectivity and positioning, emergency services, IoT, and different future location aware services such as proactive radio resource management (RRM), among others [14]. 3GPP has incorporated NR-based positioning in the latest 5G specifications, which emphasizes the importance of positioning in 5G [2]. Due to the advanced new features in 5G such as high carrier frequencies, large bandwidth, a substantial number of antenna array elements, and network densification, it is possible to achieve higher positioning accuracy using existing infrastructure and with little to no extra additional resources [15]. This positioning scheme is typically performed by the

timing-based, angle-based, or hybrid techniques. The general concept of 5G NR positioning is portrayed in Figure 3.

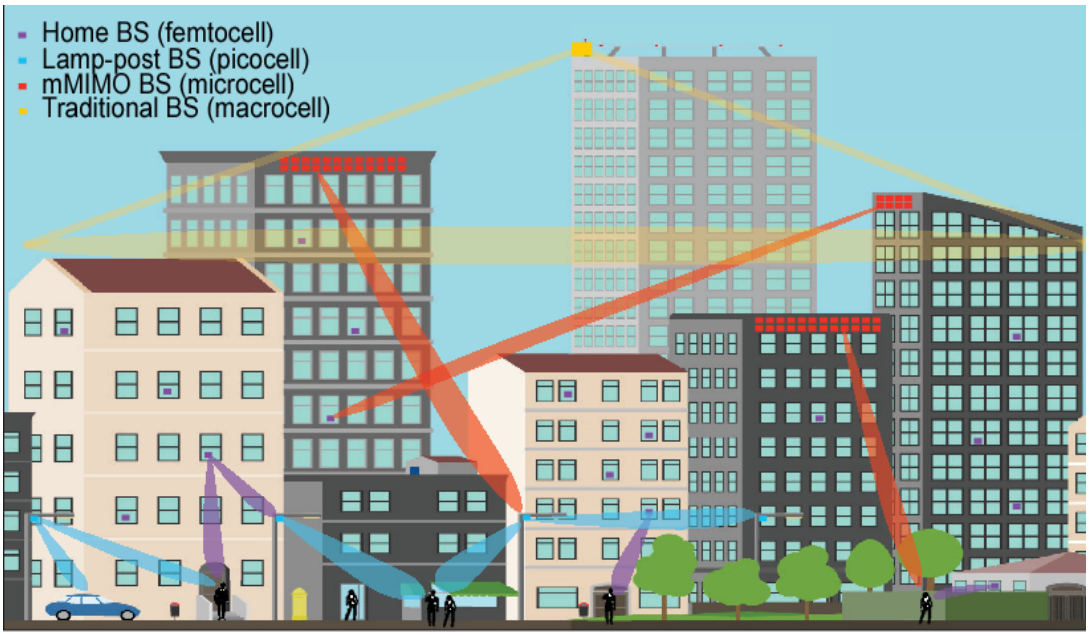

Figure 3 *General concept of 5G NR positioning* [16]

5G NR will utilize millimeter wave (24 GHz and above) bands, but due to the high amount of path loss in this band, modern technologies such as highly directional antenna, beamforming will be used. MmWave frequencies typically require LOS between user and base stations due to the losses mentioned above and network densification is one way of achieving that. These features relating to mmWave frequency will pave the way for developing high-precision positioning solutions. Due to the availability of large bandwidth in 5G NR, the TOA estimation for user positioning will be more precise due to large bandwidth enables high resolution in time-domain sampling. Owing to very small millimeter level wavelength, it is possible to pack a high number of antenna elements in a small area, which will provide the possibility of highly directional beamforming capability, and usage of large antenna arrays will drastically improve the AOA estimation for user positioning. The higher TOA and AOA estimation accuracy generally result in higher positioning accuracy. Network densification signifies a high density of base stations in 5G NR. Because of that, a user can connect to multiple base stations, which will provide higher data rates, less power consumption of the user devices, and lower latency. If the position of base stations is known, then an ultra-dense network can mean high-accurate positioning, due to the fact that positioning accuracy depends highly on diversity, number of base stations, and geometry between transmitter and receiver [15].

2.2 Different Positioning Methods

Positioning in general terms means finding out the location of a particular object by comparing typically the distance, angle, or signal power between the object and the reference point. The reference can be a single object or multiple objects. In earlier days positioning was determined with the help of known landmarks, such as mountains, trees, location of the star or the sun, etc [17]. The discovery of radio waves in the late nineteenth century has made radio-based navigation achievable. The radio waves have far longer propagation distance than visible distance and able to travel through clouds or fogs or can propagate as a ground wave over a long distance. Knowledge about a user's or a mobile terminal (MT) location can be used in several ways. The most well-known applications for positioning systems are currently the navigation services for both the customer and professional markets. The positioning solutions offered can be divided into categories. Those are, positioning: determine solely the location of an object, tracking: monitoring the movement of an object, and navigation: routing and guidance from one place to another.

There are many different ways of determining the position of an object. The reference points can be ground based or satellite based, technologies used for positioning could be different, a method of determining the location of the object could also be separate. Based on the above-mentioned points, positioning can be divided into three major systems. These are ground based positioning system, satellite based positioning system, and wireless communication-based positioning system.

2.3 Ground Based Positioning System

Before the Satellite based positioning system became mainstream, radio signals transmitted from terrestrial stations were used for positioning purposes. There are certain challenges to implement ground based positioning system. Making a formation of dense radio beacons is expensive, and in some cases even impossible. For example, to cover the maritime areas, radio transmitters have to cover a relatively wider area. Long waveband radio signals are well suited for covering wide areas and signals mainly propagate as ground waves, that is, the electromagnetic waves follow the Earth’s surface [18]. This allows for determining the propagation distance of the signal by measuring the propagation delay for accurate ranging [19]. In order to ensure wide coverage, the terrestrial wide area radio positioning system operates at 30 kHz to 300 kHz long wave band. DECCA, LORAN, and OMEGA are some well-known example of ground based positioning system [17].

2.4 Satellite Based Positioning System

Satellite positioning is the most widely used positioning system in our society. GPS is probably the most well-known representative of today's GNSS. Apart from GPS, there are other Satellite navigation systems in operation, currently planned, or being built. These are the Russian Global Navigation Satellite System (GLONASS), the Chinese Beidou system, European Galileo system, Indian Regional Navigational Satellite System (IRNSS), and Japanese Quasi-Zenith Satellite System (QZSS). The GPS, GLONASS, and Galileo use the TOA approach to determine the position of the object [20]. This approach requires precise time measurements; for these reasons, atomic clocks are placed on each satellite for precise clock synchronization. The receiver calculates three coordinates in the space domain and as a fourth parameter the navigation system time reference from the received signal. Thus, there are four unknowns that can be determined using four equations. Therefore at least four satellites are required to determine a position [21].

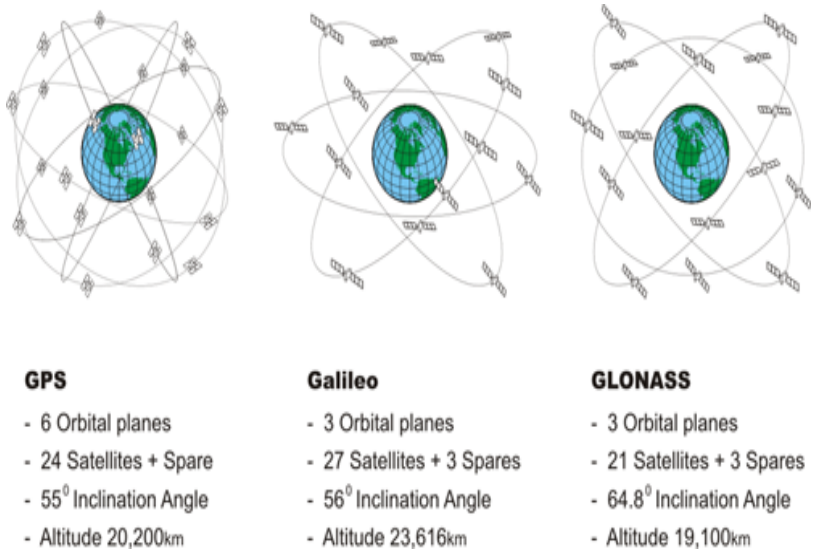

Figure 4 *GNSS satellite orbits* [22]

The three major satellite navigation systems GPS, GLONASS, and Galileo operate in medium earth orbits (MEO) as illustrated in Figure 4. The number and distribution of the orbits of the satellites as well as the number of satellites within each orbit differ between these systems. The positioning accuracy for different GNSS services such as GPS is around 2-5 meters [1] and in indoors and tunnels, the services are degraded even more as GPS satellites mainly communicate with the device via LOS communication.

2.5 Wireless Communication Based Positioning System

Wireless communication based positioning utilizes the existing telecommunication infrastructure to provide positioning services for users. Based on where the location determination is carried out, positioning can be divided into two approaches. In the self-positioning, the position of the user is calculated at the device with the help of received signal from the transmitter of known position. In network-positioning, a signal is transmitted by a transmitter unit at an unknown position and received by a receiver of known position. The position is then calculated at the network [23]. There are many different ways of determining user position. Some of them are based on propagation time principle such as TOA, Time Difference of Arrival (TDOA), Round-Trip Time of Arrival (RTTOA), etc, some of them are based on the arrival angle of the received signal, for instance, AOA, and some of them are based on transmitted signal characteristics or fingerprinting, like cell-ID based positioning, received signal strength (RSS) based positioning, power delay profile (PDP) positioning among others [24].

2.5.1 Time of Arrival (TOA)

The TOA-based positioning determines the user position by measuring the signal propagation delay to measure the distance between the transmitter and the receiver as shown in Figure 5. However, to measure the distance from the propagation delay, one assumption has to be made, the electromagnetic wave propagates along the shortest path with no reflection, refraction, or deflection [25]. If d_i is the propagation distance between the user and base station (BS_i) then [17],

$$d_i = \int d_s = \int_{T_o}^{T_i} c dt = c(T_i - T_o) \quad (1)$$

Here, T_0 is the time of transmission, T_i is the time of reception and c is the speed of light. We have assumed LOS propagation, for that the distance d_i determines points of equal distance between the BS_i and MT. This is similar to a circle with a radius of d_i and BS_i as the center in two dimensions. In three dimensions, d_i and BS_i represent the radius and center of a sphere. To determine the unique position, the distance between several BS and MT has to be measured. Moreover, the intersection of those corresponding circles will provide the unique position of the MT. If we consider, two BS, then the intersection between two corresponding circles provides two possible positions, and the addition of a third base station allows determining the truly unique position in the case of two dimensions as can be seen from Figure 5. If we consider the MT position to be determined is (x, y, z) then [26],

$$\sqrt{(x-x_1)^2+(y-y_1)^2+(z-z_1)^2} = c(T_1 - T_o) = d_1$$

$$\sqrt{(x-x_2)^2+(y-y_2)^2+(z-z_2)^2} = c(T_2 - T_o) = d_2 \quad (2)$$

$$\sqrt{(x-x_3)^2+(y-y_3)^2+(z-z_3)^2} = c(T_3 - T_o) = d_3$$

$$\sqrt{(x-x_N)^2+(y-y_N)^2+(z-z_N)^2} = c(T_N - T_o) = d_N$$

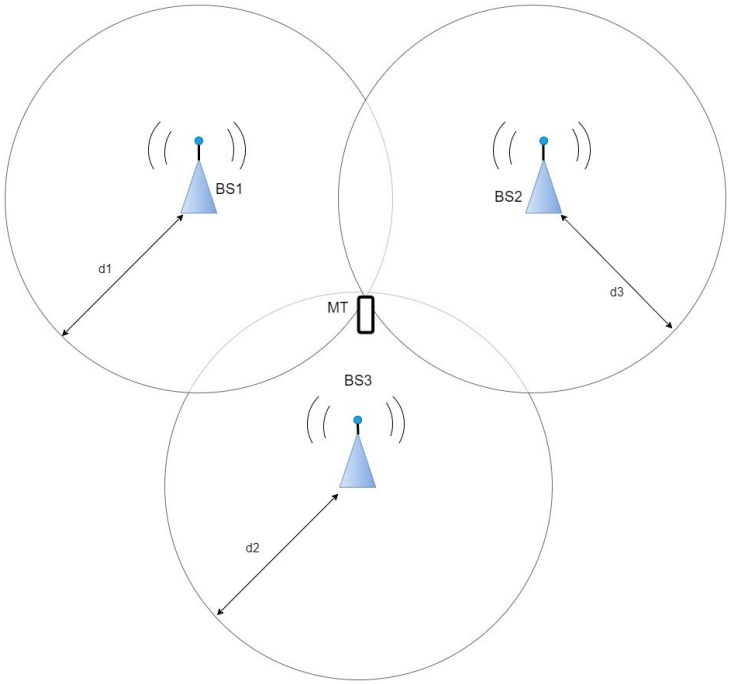

Figure 5 *General principle of TOA-based positioning in a two-dimensional case*

Here, (x_i, y_i, z_i) are the known position of BS_i. For determining the two-dimensional coordinates (x, y) or three-dimensional coordinates (x, y, z) of the MT position we would require corresponding two or three equations. However, because of the nonlinear properties of the equations, one more equation is required to resolve ambiguous solutions.

There are some drawbacks to TOA estimation. In order to obtain exact propagation delay, the time at all the BS and MT has to be exactly the same, which is hard to achieve, and for that high-accuracy synchronized clocks are required at BS and MT. Also, in practice, the distance measurement d_i is noisy and there are no unique solutions for the equation (2). Additionally, NLOS conditions caused by reflection, refraction, or diffraction is also another major source of error in determining the distance. In order to mitigate these shortcomings, combining TOA with other positioning technologies have been proposed in different usage scenarios [26][27].

2.5.2 Time Difference of Arrival (TDOA)

Similar to TOA based positioning, the TDOA based positioning also utilizes the signal propagation delay to determine the user position. TDOA measures the signals propagation delay differences between multiple base stations . Due to the employed propagation delay differences, the common term T_0 in (2) can vanish and hence also possible synchronization error between the MT and the base stations can be cancelled out from the TDOA-based positioning equations [28]. The general principle of TDOA based positioning is illustrated in Figure 6. If we consider two signals are transmitted from BS_1 and BS_2 simultaneously at time instance T_0, and the receiver

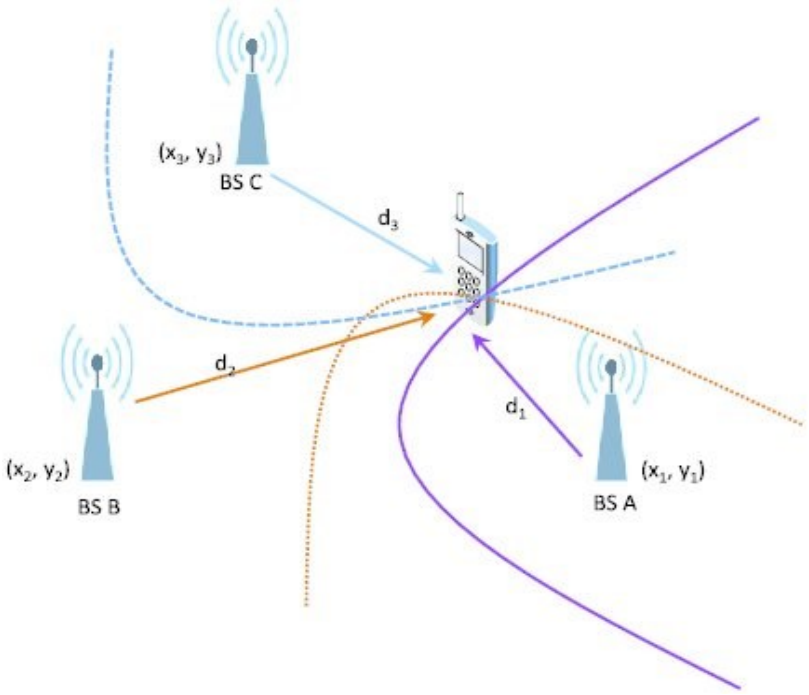

Figure 6 *General principle of TDOA-based positioning in a two-dimensional case* [17]

receives the signal from BS_1 and BS_2 at time instances T_1 and T_2 respectively. The corresponding propagation distance difference can be determined by the equation (3) [29],

$$d_2 - d_1 = c(T_2 - T_0) - c(T_1 - T_0) = c(T_2 - T_1) \tag{3}$$

Both time instances T_1 and T_2 used for calculating the signal propagation delay difference are measured at the MT. Therefore, the possible MT synchronization error between MT and BSs can be cancelled out assuming that the network elements are mutually synchronized. Contrary to the TOA based positioning, a signal propagation delay difference measurement of TDOA defines points of equal distance differences to the corresponding base stations It is the characterization of a hyperbola in the two-dimensional case or a hyperboloid for the three-dimensional space. For this reason, the TDOA is also called hyperbolic positioning. Hyperbolas with foci at the positions of the concerned base

stations mark the geometric points of equal distance difference to those base stations. The intersection of these different hyperbolas, or hyperboloids in the three-dimensional space, provide the MT position. If there are N base stations, then N-1 nonlinear TDOA equations are given in (4).

$$\begin{aligned}&\sqrt{(x-x_2)^2+(y-y_2)^2+(z-z_2)^2}-\sqrt{(x-x_1)^2+(y-y_1)^2+(z-z_1)^2}=d_2-d_1\\&=c(T_2-T_1)\end{aligned}$$

$$\begin{aligned}&\sqrt{(x-x_3)^2+(y-y_3)^2+(z-z_3)^2}-\sqrt{(x-x_1)^2+(y-y_1)^2+(z-z_1)^2}=d_3-d_1\\&=c(T_3-T_1)\end{aligned}$$

$$\begin{aligned}&\sqrt{(x-x_N)^2+(y-y_N)^2+(z-z_N)^2}-\sqrt{(x-x_1)^2+(y-y_1)^2+(z-z_1)^2}=d_N-d_1\\&=c(T_N-T_1)\end{aligned} \tag{4}$$

Here (x, y, z) denotes the unknown position of the MT and (x_i, y_i, z_i) denotes the position of BS_i. Compared to the TOA method, one less equation is required to determine the MT's position and thus less computational power is required for position estimation. Similar to TOA, the propagation path of TDOA estimation is assumed to be LOS. However, if there is NLOS propagation, the position of reflectors or obstacles causing refraction or diffraction has to be known. Otherwise, these positions are further extra unknown variables in the system of TDOA equations. In addition to standalone TDOA based positioning, hybrid TDOA and AOA or RSS and other technologies have also been proposed based on different requirements and positioning scenarios [30][31].

2.5.3 Angle of Arrival (AOA)

In AOA positioning principle, the positioning of the user is determined by the direction in which the signals arrive at the receiver. The AOA method theoretically can be applied for both uplink and downlink. At first, let us consider two dimensional MT location for AOA measurement in the downlink. Measurement for the location of each base station (x_i, y_i) and direction φ_i provides a straight line defining possible locations of the MT in LOS conditions and the intersection of those straight lines between two base stations provides the unique location of the MT as shown in Figure 7. If we consider the polar coordinate system, then for each BS_i, we get [32],

$$(x - x_i) = r_i \cos(\varphi_i)$$

$$(y - y_i) = r_i \sin(\varphi_i) \tag{5}$$

which can be rewritten as

$$(y - y_i) = \tan(\varphi_i)(x - x_i)$$

Thus, in order to determine the position of the MT (x, y), we need to solve the following two equations.

$$(y - y_1) = \tan(\varphi_1)(x - x_1)$$

$$(y - y_2) = \tan(\varphi_2)(x - x_2) \tag{6}$$

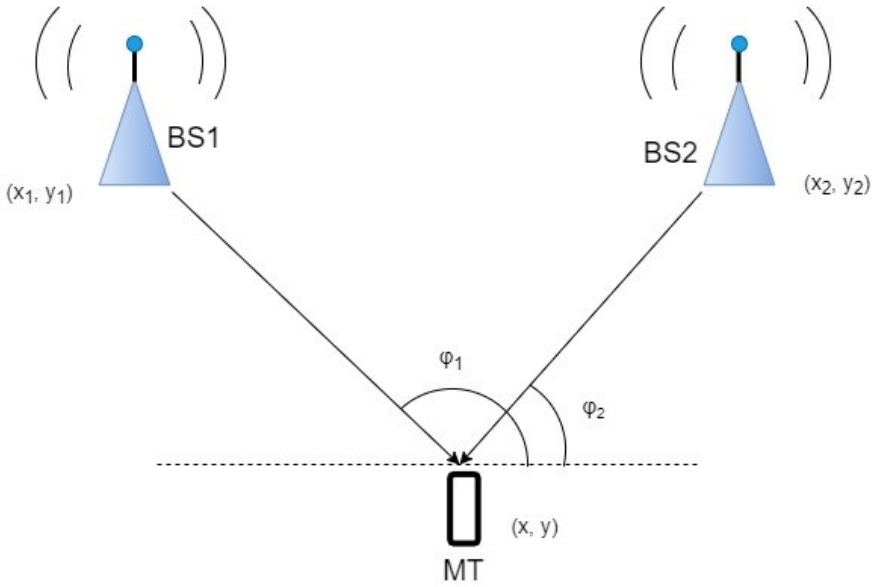

Figure 7 *General principle of AOA based positioning in two dimensions*

However, in downlink AOA measurement, the orientation of MT antennas will also have to be considered to achieve correct position estimation. It can be typically obtained from the Inertial Measurement Unit (IMU) sensors, which is very challenging as the position and orientation is dynamic and can be considered always changing.

For AOA application in the uplink, the AOA values are determined at the base stations and the orientation sensitivity is not as severe as AOA in the downlink. In general, the BSs are fixed in their position and It can be plausibly assumed that the orientations of the receivers or the base stations are known quantities. Additionally, the number of antenna array elements for downlink AOA is restricted due to the size of the MT, however, at the base station end the size or number of antenna elements is less of an issue and it is easy to achieve better directional resolution [33].

There are some limitations to the AOA technique especially during NLOS propagation. During NLOS propagation, the signal received at the BS antenna array is reflected and results in deviated AOA than the direction of the MS. Due to these phenomena, the accuracy of AOA decreases with the increasing distance between MT and BS [34]. Moreover, when the MT is along the straight line between two BSs, it is not possible to determine the MT location with AOA principle. In order to address these shortcomings and improve the positioning accuracy, combination of AOA and other positioning technologies have been utilized or proposed in different positioning applications [35][31].

2.5.4 Cell-ID

Cell-ID based positioning utilizes the principle of fingerprinting. A fingerprint in wireless positioning is the set of measurable signal characteristics that depend on the position of transmission or reception. The basic principle of the Cell-ID based position is delineated in Figure 8. Each BS broadcasts both the Location Area Identity (LAI) and the Cell-ID to its corresponding cells and the MT is always listening to these broadcast messages [36]. If the signal of a BS is present for a particular MT, then the location of the MT is within the serving radius of that particular BS. Each BS has a unique cell-ID and by identifying the cell-ID it is possible to locate the general location of the MT.

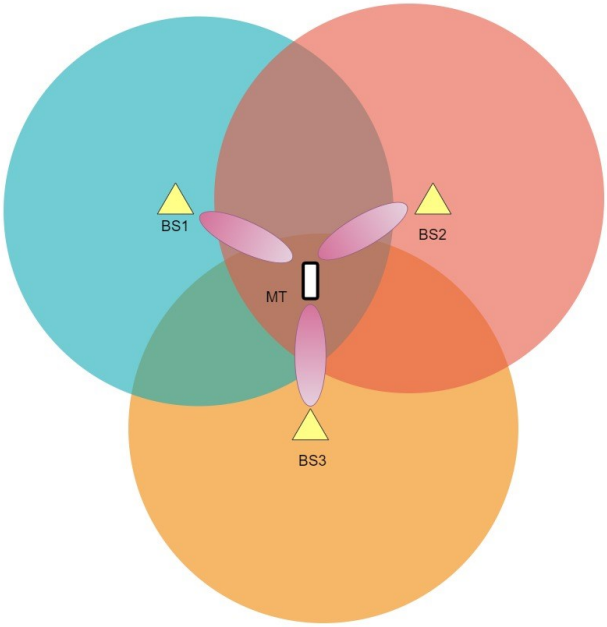

Figure 8 *Basic principle of Cell-ID based positioning*

The size and shape of this area depend on the cell area and shape and can be determined through measurement [17]. Let us consider an MT within the coverage area of three base stations. The MT receives signals from all three of them and the only information, which is required from the signal, is the ID of the MT that is transmitting the signal

and the position of the MT must be within the coverage areas of all three base stations at the same time. Therefore, the position of the MT will be within the common coverage area of these three base stations [37]. On top of the Cell-ID based positioning, there is also enhanced cell-ID based positioning that utilizes the MT and RAN radio resource related measurements to further enhanced the localization accuracy [34]. The positioning accuracy of cell-ID positioning depends on several factors. These are the size of the base station coverage area, the number of received base stations, and the reliability of their determination [17]. Additionally, combination of Cell-ID and other technologies have also been proposed to provide reliable and improved positioning accuracy in different positioning scenarios [38][39].

2.5.5 Received Signal Strength (RSS)

RSS is a fingerprint principle based positioning method. In cell-ID positioning, the signal power of the received signal is classified as binary, which is whether or not the signal is present. Further quantization of the received signal is what the RSS principle is based on. However, the achievable size of the quantization is limited by the receiver hardware, particularly the analog-to-digital converter. In general, the average received signal power is inversely proportional to the distance between the transmitter and the receiver. Therefore, based on the received signal power it is possible to determine the distance between the base station and the MT [40].

$$P_{RX} \propto P_{TX} G_{Tx} G_{Rx} \left(\frac{d}{d_0}\right)^{-\beta} \tag{8}$$

Here, P_{RX}, P_{TX}, G_{TX}, G_{RX}, d_0, d and β denote the received signal power, transmitted signal power, transmitter antenna gain, receiver antenna gain, reference distance, the Euclidean distance between transmitter and receiver, and decay factor respectively. The values of these parameters have to be estimated to absolutely measure the position of the MT [41]. The problem associated with unknown proportionality constant is present for database-supported RSS positioning. The problem can be raised from that a RSS database is usually developed using some measurement equipment and used later on for positioning by lots of different MTs. The scaling of the RSS database values must be the exact same for both the measurement device and the MTs that use that database for positioning. Furthermore, the main drawback of RSS bases positioning is that it depends on many unpredictable and changeable factors such as path loss, different propagation environments, multipath phenomenon etc [42].

2.5.6 Different Indoor Positioning Technologies

Indoor positioning systems provide real-time positioning and continuous tracking solutions for persons or objects in indoor environments. Indoor positioning is quite different compared to outdoor positioning in some key characteristics. The indoor structure is typically more complex, and objects such as walls, equipment, furniture, peoples for instance are more densely arranged. Due to that, the signals are reflected and leading to more severe multipath scenarios. Also, due to complex indoor structures, devices usually rely on NLOS propagation to communicate with each other. Furthermore, due to the existence of frequent obstacles, the signals are attenuated and scattered heavily. Another key difference between indoor and outdoor positioning is due to the relatively smaller areas and multiple floors higher vertical and horizontal accuracy and precision are required compared to outdoor environments. There are different indoor positioning technologies available currently such as Wireless Local Area Network (WLAN) based, Bluetooth based, Ultra Wide Band (UWB), Zigbee, Radio Frequency Identification (RFID), Infrared based, among others. Brief description of UWB based, Wireless Fidelity (WIFI) based, Bluetooth low energy (BLE) based, and RFID based indoor positioning systems are given below.

UWB is defined as the RF signal having fractional bandwidth greater than 20% or bandwidth equal to or greater than 500 MHz, regardless of the fractional bandwidth [43]. UWB transmits signals over a wide spectrum which allows transmitters to transmit a large amount of data at the cost of very little energy. For this reason, UWB is a promising solution for ultra-low power and precise indoor positioning applications. UWB system requires several anchors working as reference whose position has to be known and then it can utilize the Two Way Ranging (TWR) principle, TDOA principle, TOA principle, among others to measure the distance between the object and the references [26][44].

IEEE 802.11 is believed to be the primary local wireless networking standard, utilizing a typical gross bit rate of 11, 54, or 108 Mbps and a range of 50 to 100 m. Similar to UWB based positioning, the location of the WLAN access points has to be known in order to use WIFI for indoor positioning. The WLAN based positioning typically utilizes the RSS principle by measuring the signal strength for positioning as it is easy to extract from 802.11networks and can be used on readymade off the shelf hardware [45]. TOA, TDOA, AOA measurements are typically not used here because of the NLOS propagation in the indoor environment, angular measurement complexity, and time delay not providing accurate distance measurement due to signal reflection.

BLE is another indoor positioning technology currently being used. Bluetooth operates in the 2.4 GHz ISM band, is one standard for Wireless Personal Area Network (WPAN) and is designed to provide very low power peer to peer communication. Compared to WLAN, Bluetooth consumes less power, has less gross bit rate, and provides a comparatively shorter range of about 10 cm to 10 m. Similar to WLAN based positioning, BLE based positioning also uses the RSS principle for object localization [46]. An example of BLE based patient monitoring and asset tracking is illustrated in Figure 9.

Figure 9 *Patient monitoring and asset tracking using BLE* [44]

RFID uses radio waves to transmit the unique identity and other information of an object. It is a promising technology for indoor positioning. A standard passive RFID system consists of two parts: the RFID reader, and the passive tag. When the RFID reader is within the range of the tag, it receives power from the reader signal and uses this power to transmit back the information stored inside to the reader [47]. The RFID-based positioning techniques can be implemented in two ways: tag-oriented and reader-oriented. In tag-oriented technique, the RFID readers are placed in certain known locations and when a certain tag is detected by any of the reader, the location and identification of the object is determined by the stored information within the tag. In reader-oriented technique the operation is similar and only difference is the tags are stationary and the readers are moving [48].

2.6 Positioning Requirements in 5G

5G system aims to provide flexible and diverse positioning services based on different environments, services, and requirements. The key parameters of positioning services are accuracy, positioning service availability, latency, energy consumption, updated rate,

time to first fix (TTFF), etc. These parameters can be configured to provide suitable positioning services to the users, corporate customers, and others [46]. In addition to providing stand-alone positioning, 5G will also support a combination of other 3GPP Radio Access Technologies (RAT) and non 3GPP positioning technologies such as GPS, GLONASS, Galileo, Terrestrial Beacon Systems (TBS), WLAN/Bluetooth based positioning, etc to achieve better accuracy and performance. These combinations could be adjusted and varied over time to achieve suitable positioning performance and energy efficiency. In addition to that, the MTs would have the ability to share the positioning information with other MTs or to the controllers [49]. 3GPP has set vertical and horizontal positioning accuracy requirements for different positioning service levels and environments. These requirements are described in Table 1. There are in total of 7 service levels defined by the 3GPP with horizontal accuracy level ranging from 0.2 m to 10 m and vertical accuracy level ranging from 0.2 m to 3 m. Additionally, each service level supports different maximum allowable positioning service latency ranging from 10 ms to 1s and different positioning service area requirements at both indoor and outdoor environments for stationary and moving objects. These service levels are described in Table 1.

These different positioning service levels are suitable for diverse positioning requirements. For example, in the use cases where a higher degree of positioning accuracy and lower latency are required such as collision avoidance of vehicles, different emergency services, etc, a higher positioning service level should be implemented [46].

Table 1 *Positioning requirements in 5G* [50]

Positioning Service Level	**Horizontal Accuracy**	**Vertical Accuracy**	**Positioning service latency**	**5G positioning service area**
1	10 m	3 m	1 s	Indoor - up to 30 km/h Outdoor (rural and urban) up to 250 km/h
2	3 m	3 m	1 s	Outdoor (rural and urban) up to 500 km/h for trains and up to 250 km/h for other vehicles
3	1 m	2 m	1 s	Outdoor (rural and urban) up to 500 km/h for trains and up to 250 km/h for other vehicles
4	1 m	2 m	15 ms	Indoor - up to 30 km/h
5	0.3 m	2 m	1 s	Outdoor (rural) up to 250 km/h
6	0.3 m	2 m	10 ms	Outdoor (dense urban) up to 60 km/h and indoor up to 30 km/h
7	0.2 m	0.2 m	1 s	Indoor and outdoor (rural, urban, dense urban) up to 30 km/h Relative positioning is between two MTs within 10 m of each other

3. 5G REFERENCE SIGNALS

In this chapter, the 5G NR frame structure, description of 5G reference signals, their functionality, and time and frequency domain resource allocation have been presented. This chapter comprises of three sections: (i) 5G NR frame structure, (ii) 5G downlink reference signals, and (iii) 5G uplink reference signals.

3.1 5G NR Frame Structure

5G NR incorporates Orthogonal frequency division multiplexing (OFDM) as the waveform for both uplink and downlink transmission. OFDM allows each carrier to be divided into multiple orthogonal subcarriers. NR permits different subcarrier spacings and not just 15 kHz as specified in LTE. The value of subcarrier spacing can be 15 kHz or power of 2 multiple of 15 kHz and up to 240 kHz. As a direct consequence, the symbol duration also changes by a factor of 2, 4, 8, or 16 for the highest subcarrier spacing. There are certain advantages of higher subcarrier spacings. For example, higher subcarrier spacing allows for higher mobility due to the ability to cope with a higher Doppler shift and also shortens the transmission time and therefore decreases the latency in the physical layer. The different subcarrier spacing, their corresponding symbol durations, maximum bandwidths (BW), and the number of slots in a subframe are shown in Table 2 [6]:

Table 2 *5G NR supported subcarrier spacing and corresponding symbol duration, Max BW, and number of slots*

Subcarrier Spacing (kHz)	15	30	60	120	240
Symbol duration (us)	66.7	33.3	16.6	8.33	4.17
Max BW (MHz)	50	100	200	400	400
Number of slots in a subframe	1	2	4	8	16

Due to the various slot structures, the frame structure is also varying in 5G NR. However, irrespective of the subcarrier spacing each resource block consists of 12 subcarriers and each slot consists of 14 OFDM symbols [51]. Each NR frame is 10 ms long and divided into two 5 ms half frames. Each half-frame consists of five 1 ms subframes and depending on the subcarrier spacing, there can be at least 1 slot or up to 16 slots per subframe. The NR frame structure for 15 kHz subcarrier spacing is shown in Figure 10:

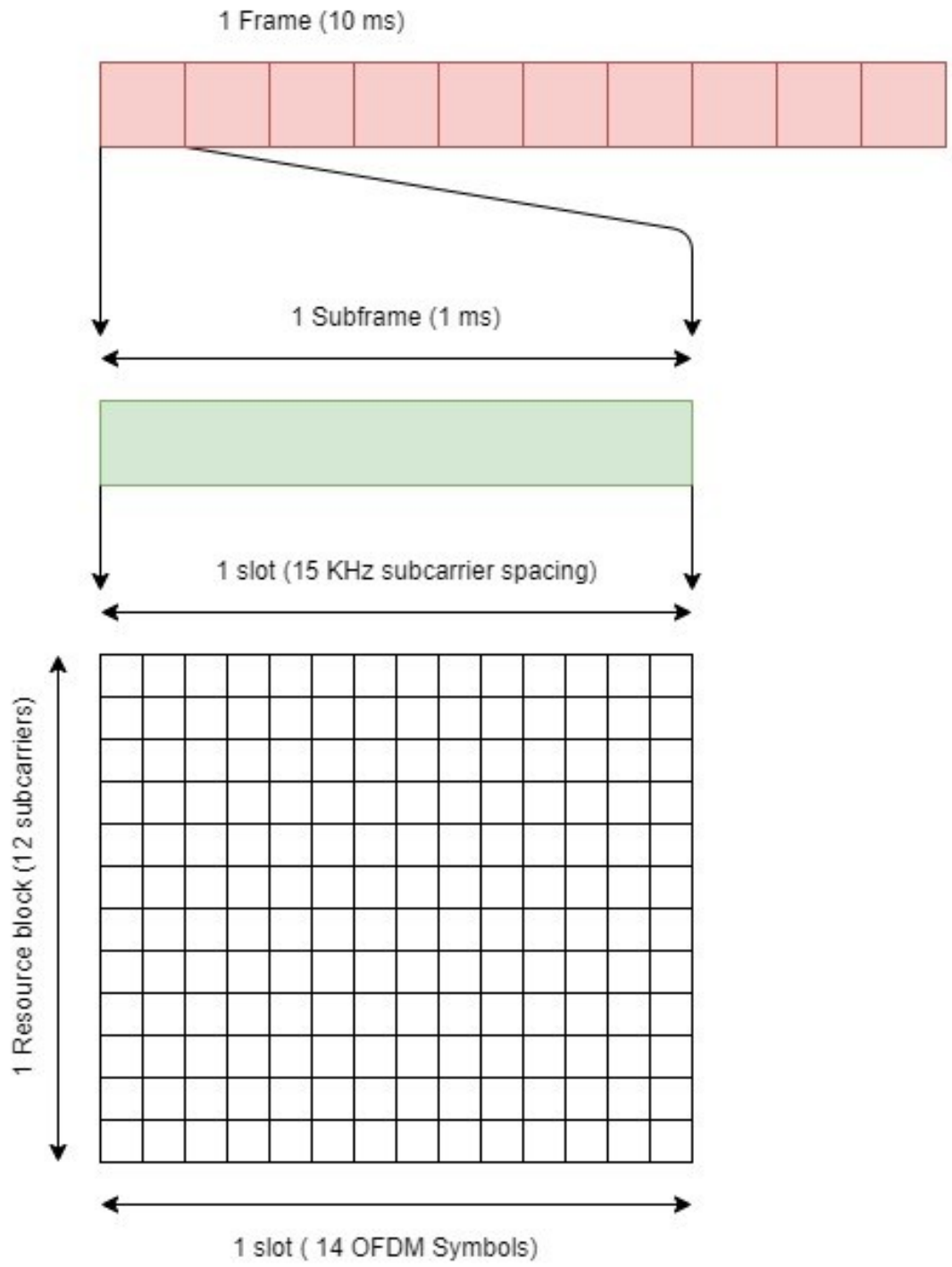

Figure 10 *5G NR frame structure*

The small block taking one subcarrier spacing in the frequency domain and one OFDM symbol in the time domain is called a resource element. All the downlink and uplink physical channels take up a set of resource elements for carrying information.

3.2 Downlink Reference Signal

The downlink reference signals are transmitted from BS to MTs for downlink channel estimation, initial access, and synchronization purposes, for instance. There are five different 5G downlink reference signals and descriptions of these signals are given in the following part of the work:

3.2.1 Demodulation Reference Signal

The demodulation reference signal is a type of downlink reference signal used for downlink channel estimation as a part of coherent demodulation at the device end. DMRS is MT-specific, can be transmitted with or without beamforming, transmitted in a scheduled manner, and transmitted only when necessary [6]. DMRS is only present in resource blocks intended for Physical Downlink Shared Channel (PDSCH) transmission.

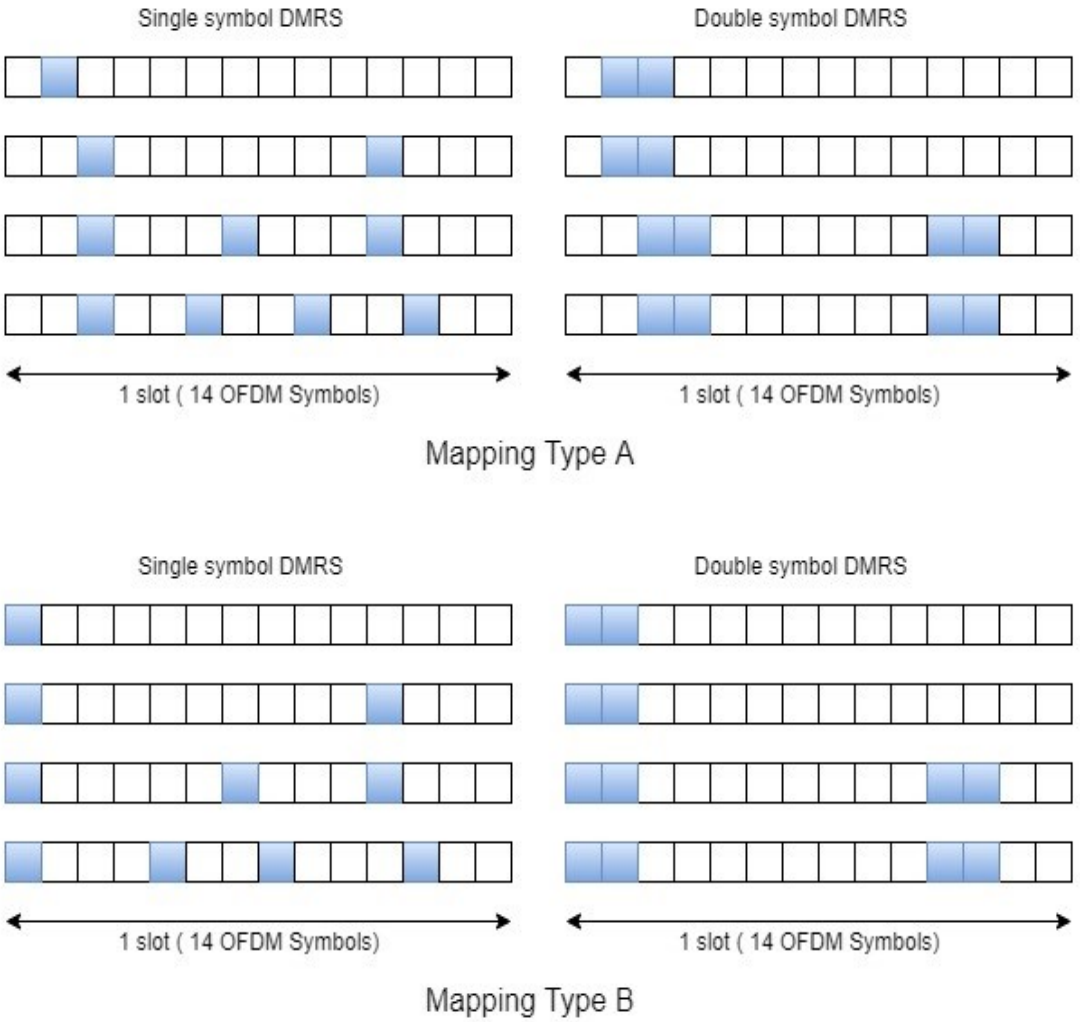

Figure 11 *Different time domain configuration of DMRS*

It is important to locate the DMRS early in the transmission, which enables the receiver to obtain the channel estimate early and process the received signal accordingly [52]. Although this front-loaded design is beneficial for low latency channel estimation, in the case of a rapid channel variation, it is possible to configure up to three DMRS occasions in an OFDM slot. The DMRS in NR provides a good amount of flexibility to be deployed in different scenarios and use cases. It supports up to 12 orthogonal antenna ports for MIMO and beamforming purposes, and transmission durations from 2 to 14 symbols and up to four symbols per slot to support rapid scenarios as shown in Figure 12. In terms of a PDSCH allocation, the DMRS can be classified into type A and type B. Type A implies that DMRS are located in the second or third symbol of a slot, right next to a Control Resource Set (CORESET) located at the beginning of the slot and type B implies that DMRS is located in the first symbol of the data allocation [6].

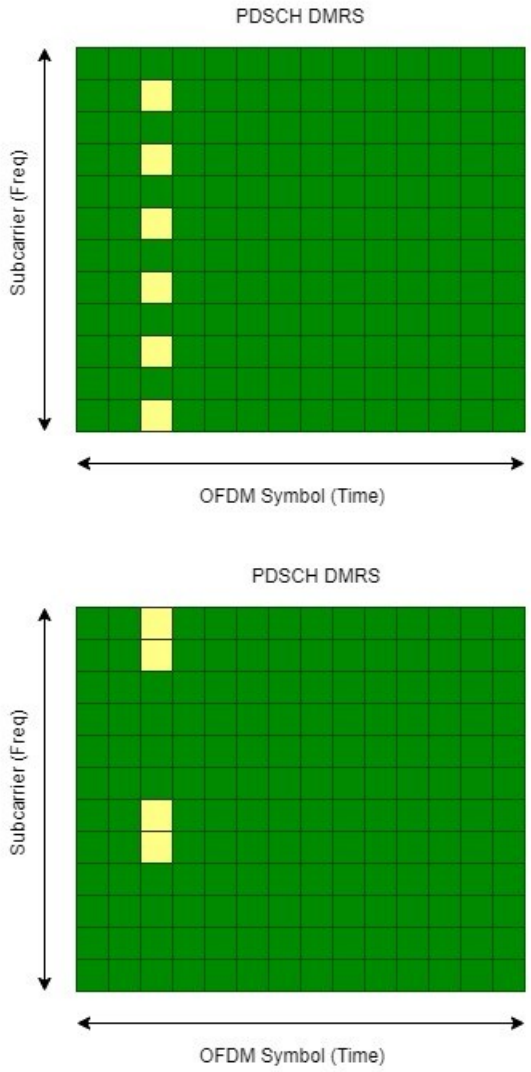

Figure 12 *Type 1 (above) and Type 2 (below) DMRS*

Based on the number of possible orthogonal sequences and density in the frequency domain, DMRS can be divided into type 1 and type 2 DMRS sequences. Type 1 corresponds to the allocation, where every other resource element in the frequency domain of the resource block is occupied by a DMRS symbol. Type 2 corresponds to the allocation, where two consecutive resource elements are occupied by DMRS symbols out of each group of six resource elements in the frequency domain of the resource block. Moreover, in terms of time domain allocation of DMRS symbols, they are divided into single-symbol and double-symbol DMRS as can be seen in Figure 11.

3.2.2 Channel State Information Reference Signal

Channel sounding refers to gaining knowledge about radio channel path loss for transmission power adjustment, and detailed awareness about channel amplitude and phase in the time, frequency, and spatial domain [6]. This channel sounding is performed by the CSI-RS in the downlink. CSI-RS are transmitted within a bandwidth part, but they are not limited to the subset of the bandwidth part that contains data for the MT- if there is any data transmission. Therefore, they can provide information about the channel across the whole bandwidth part, contrary to DMRS associated with the data transmission. CSI-RS may be configured for up to 32 different antenna ports, each assigned to a channel to be sounded and thus allows to be beamformed [53]. One example structure of 32 antenna port configuration is depicted in Figure 13.

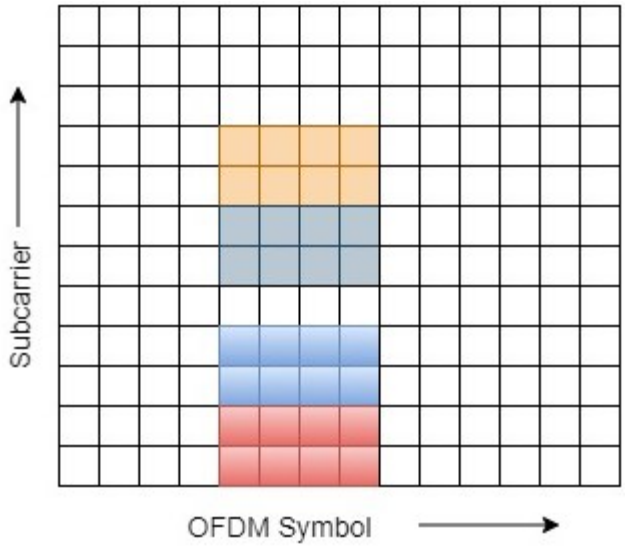

Figure 13 *One structure of 32 port CSI-RS*

A single-port CSI-RS takes a single resource element of a resource block. In terms of the CSI-RS density in the frequency domain, they are divided into two types. If the CSI-RS is configured to be transmitted in every resource block, then it is called to have a

CSI-RS density one and if CSI-RS is configured to be present in every second resource block, then it is called CSI-RS density half. In the latter case, the CSI-RS configuration specifies within which resource blocks (odd or even resource blocks) the CSI-RS will be transmitted. CSI-RS periodicity in the time domain can be divided into three different types: periodic, semi-persistent, and aperiodic. For a periodic CSI-RS transmission, a MT can be configured to receive CSI-RS information in every N^{th} slot, where N can range from 4 to 640 slots [6]. Periodic CSI-RS configuration for a different level of periodicity and slot offset is delineated in Figure 14.

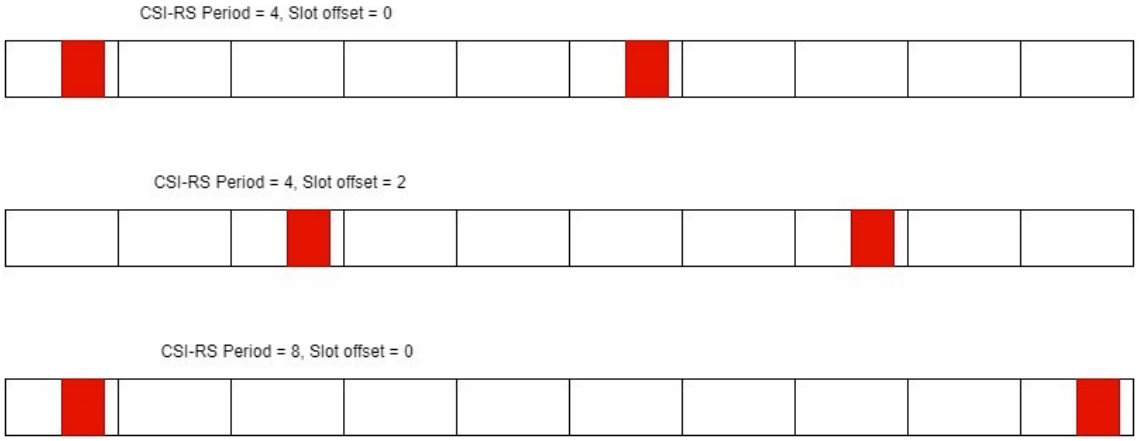

Figure 14 *Different levels of CSI-RS periodicity and slot offset*

In the case of a semi-persistent CSI-RS transmission, it is similar to the periodic transmission in terms of periodicity and slot offset, but the CSI-RS transmission can be activated or deactivated. Finally, for the aperiodic transmission, no periodicity is defined for the CSI-RS transmission, and MT has to be notified for each transmission instant with downlink control information (DCI) [6].

3.2.3 Synchronization Signal Block

When a new device tries to connect to the network, synchronization signals assist the device to find a new cell to nest. The major difference between NR Synchronization Signal (SS) blocks and corresponding LTE signals is that it is possible to transmit NR SS blocks in different beams multiplexed in the time domain. The synchronization signals consist of two parts: the primary synchronization signal (PSS) and secondary synchronization signal (SSS). They are transmitted in downlink periodically from each cell. The PSS, SSS, and Physical Broadcast Channel (PBCH) jointly form the SS block. Each SS block occupies 240 subcarriers in the frequency domain and 4 OFDM symbols in the time domain. The PSS is transmitted in the first OFDM symbol and it occupies 127 sub-

carriers from the middle of the SS block. The SSS is transmitted in the third OFDM symbol of the SS block and takes the same 127 center subcarriers. The PBCH transmission takes the second and fourth OFDM symbols and they are transmitted within the whole 240 subcarriers. Besides, PBCH is also transmitted on both sides of the SSS occupying 48 subcarriers on each side of the SSS transmission part and thus takes a combined 576 resource elements per SS block [6]. The SS block resource allocation in the time and frequency domain is illustrated in Figure 15.

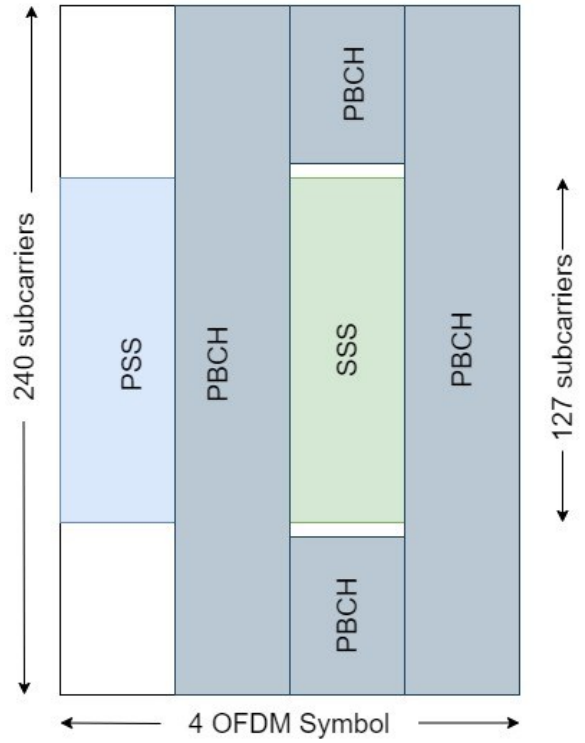

Figure 15 *SS block resource allocation in time and frequency domain*

There can be multiple SS blocks in a single half-frame depending on the frequency band. The set of such SS blocks are combinedly called an SS burst set. For frequency bands below 3 GHz, there can be up to 4 SS blocks in a single half-frame, for frequency bands between 3 GHz and 6 GHz there can be up to 8 SS blocks, and for higher frequency bands maximum of 64 resource blocks in a single SS burst can be configured [54]. Another important aspect of the SS block resource allocation is periodicity. The SS blocks can be transmitted periodically such that periodicity can vary from 5 ms to 160 ms depending on the scenario. For example, the denser SS blocks may enable faster cell search for devices in a connected mode and longer SS block periodicity may help the network achieve better energy efficiency. Table 3 shows the SS block bandwidth for different subcarrier spacings [6].

Table 3 *SS block BW in relation to the subcarrier spacing and carrier frequency*

Subcarrier Spacing in kHz	Carrier Frequency Range	SSB Bandwidth in MHz
15	FR1	3.6
30	FR1	7.2
120	FR2	28.8
240	FR2	57.6

3.2.4 Phase Tracking Reference Signal

Phase tracking reference signal (PT-RS) is a new reference signal introduced in 5G NR. The purpose of PT-RS is to track phase deviations across the transmission duration. The phase deviation is mainly caused by the phase noise introduced by the oscillators which are also known as carrier frequency offset, primarily at higher carrier frequencies. This is partially the reason behind the absence of subsequent reference signal in LTE. The PT-RS is dense in the frequency domain and sparse in the time domain as shown in Figure 16 as its main purpose is to track the phase noise [55]. The PT-RS is scheduled in combination with the DMRS and only present if the network requires the PT-RS to be present. The PT-RS is repeated in every Lth OFDM symbol in the time domain, starting with the first OFDM symbol in the allocation [6, 56].

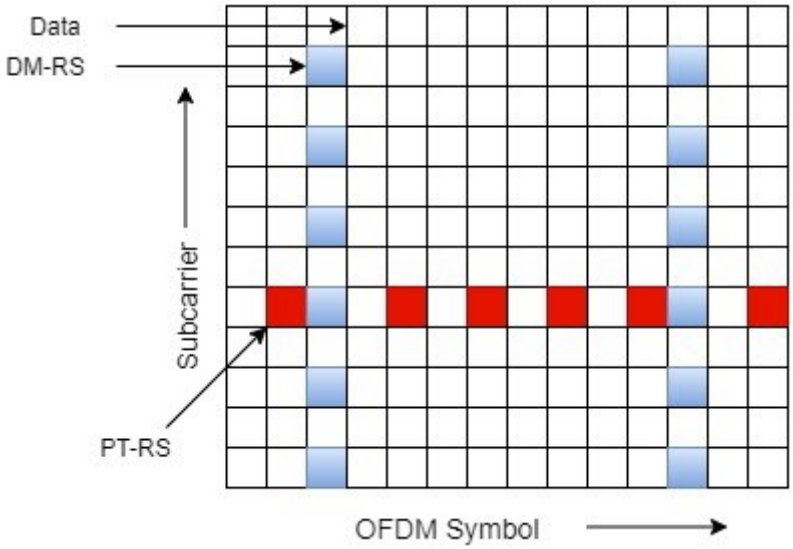

Figure 16 *PT-RS occasions in a single slot and single resource block*

The PT-RS transmission after every Lth OFDM symbol reset after each DMRS transmission as there is no need for PT-RS immediately after a DMRS occasion [5]. The density in the time domain is linked to the scheduling of the modulation coding scheme (MCS) in a configured way [6]. In the frequency domain, the PT-RS is transmitted in a very sparse manner, either in every second or fourth resource blocks. The density of PT-RS in the frequency domain is thus directly related to the transmitted bandwidth, such that the higher the bandwidth the lower the PT-RS density. But for the smallest transmission bandwidth, there is no PT-RS at all.

3.3 Uplink reference signal

The uplink reference signals are transmitted from MTs to the BS for uplink channel estimation purposes. According to the 3GPP TS 38.211 [5], there are three uplink reference signals, and their descriptions are given in the following part of the work:

3.3.1 Demodulation Reference Signal

The DMRS transmission for uplink is similar to the downlink transmission, and uplink DMRS is only present in resource blocks intended for Physical Uplink Shared Channel (PUSCH) transmission. The main difference is DFT-precoded OFDM for the uplink only supporting single layer transmission. The transmission of reference signals frequency multiplexed with other uplink transmissions from the same device is not ideal for uplink, because this will adversely affect the performance of the system's power-amplifier efficiency due to increased cubic metric. As DFT-precoded OFDM is capable of performing single layer transmission only and hence, there is no need for a high degree of multiuser MIMO support; it follows the same mapping configuration as type 1 in downlink DMRS transmission [57].

3.3.2 Sounding Reference Signal

The sounding reference signal is equivalent to CSI-RS in the uplink. The purpose of CSI-RS and SRS are similar but there are some fundamental structural differences between the two of them. The SRS supports only up to four antenna ports compared to 32 ports of the CSI-RS and also SRS is designed for power efficiency as it is transmitted by the MT compared to CSI-RS which is transmitted by the BS [6]. Based on the type of transmission within the bandwidth, the SRS can be categorized into two methods. The non-

frequency-hopping SRS, which is a single SRS transmission for the entire desired bandwidth, and frequency-hopping-SRS, in which the transmission of SRS is divided into a sequence of narrowband transmissions covering the entire desired bandwidth [6].

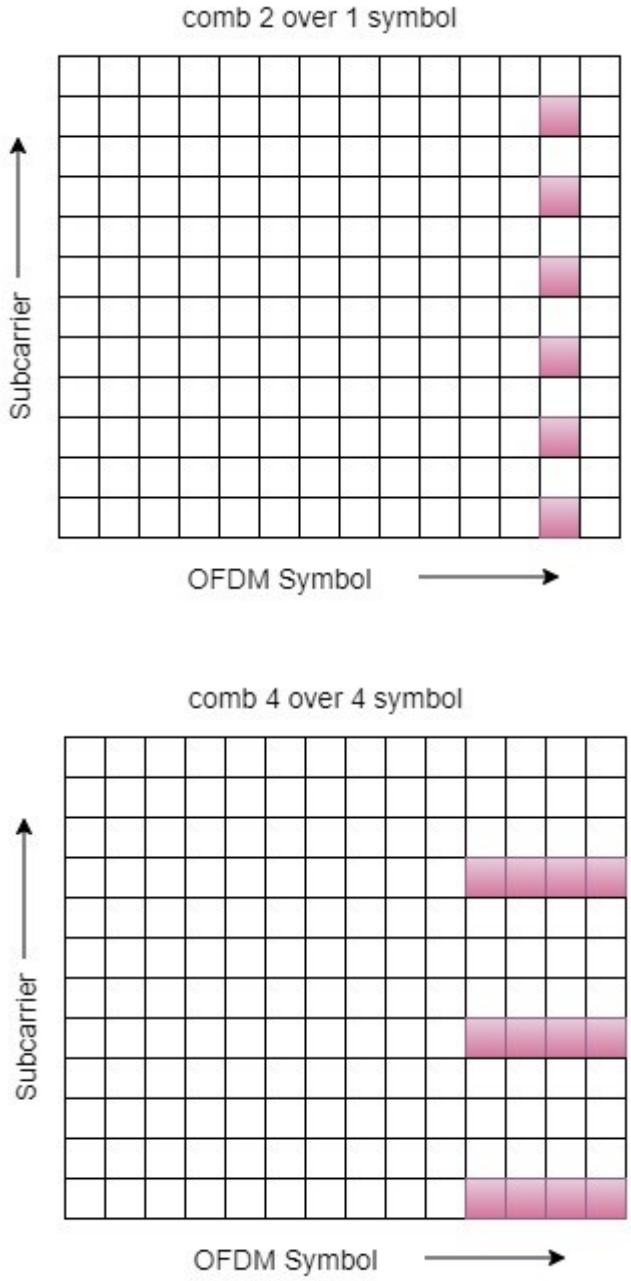

Figure 17 *Different formations of SRS structure in time and frequency domain*

In the time domain, the SRS takes one, two, or four consecutive OFDM symbols and generally located within the last six symbols of the slot. In the frequency domain, SRS follows the comb structure and transmitted in every Nth subcarrier, where N can be either two or four. Moreover, SRS transmission from different devices can be frequency multiplexed in the same resources by assigning different combs for different devices as shown

in Figure 17. For comb-2, SRS from two different devices can be frequency multiplexed and for comb-4, four SRS can be frequency multiplexed [58].

3.3.3 Phase Tracking Reference Signal

In DFT-precoded OFDM in the uplink, the PT-RS samples are inserted before the DFT precoding. The time domain allocation is the same as PT-RS in downlink as it is repeated in every Lth OFDM symbol and the counter is reset after every DMRS transmission [17].

4. POSITIONING PERFORMANCE ESTIMATION METHODOLOGY

In this chapter, the method of measuring the performance of TOA and AOA based positioning has been depicted. Additionally, the theory of measuring the geometrical influence on positioning has also been briefly described.

4.1 Method of Measuring TOA and AOA Estimation Accuracy

The TOA measurement accuracy has been calculated by taking the variance of the distance estimates. The Cramér–Rao inequality establishes a lower bound of the variance of an estimate which is the best performance any unbiased estimator can perform. The Cramer-Rao Lower Bound (CRLB) is used in this work to analyze the theoretical positioning performance in the system. We have considered the timing estimation of the OFDM multicarrier modulation scheme as it will be used in 5G [17]. If we consider signal energy is distributed equally over the subcarriers then, the CRLB of the variance of the distance estimation can be obtained as [59],

$$VAR\{\hat{t}(r)\} \geq \frac{\sigma^2}{8\pi^2 {f_{SC}}^2 |S|^2 \sum_{n=-M}^{M} n^2} = \frac{1}{8\pi^2 {f_{SC}}^2 \frac{|S|^2}{\sigma^2} \frac{M(M+1)(2M+1)}{3}}$$

$$VAR\{\hat{\tau}(r)\} \geq \frac{1}{8\pi^2 {f_{SC}}^2 SNR \frac{M(M+1)(2M+1)}{3}} \quad (9)$$

And the total occupied bandwidth is,

$$B = N_u f_{SC} \quad (10)$$

Here, f_{SC} and N_u denote the subcarrier spacing and the total number of subcarriers, respectively and M denotes the number of subcarriers symmetrically distributed around the subcarrier zero. The CRLB for distance estimation can be calculated by multiplying the standard deviation of the timing estimation with the speed of light denoted as c, such that,

$$\text{stddev} = \text{c}\sqrt{\text{VAR}\{\hat{\tau}(\text{r})\}} \cong 3 \times 10^8\, ms^{-1} \times \sqrt{\text{VAR}\{\hat{\tau}(\text{r})\}} \quad (11)$$

In regards to AOA, the CRLB for AOA estimation error magnitude can be stated as [60],

$$VAR\{\hat{\alpha}(r)\} \geq \frac{6}{\left(L(L^2 - 1)SNR\, k^2 d^2 cos^2(\alpha)\right)} \quad (12)$$

Here, L, k, d, and α denote the number of antenna array elements, wave number, antenna element separation distance, and the angle of the received signal with respect to the antenna boresight direction. If $k = 2\pi/\lambda$, and assume $d = \lambda/2$ where λ is the wavelength of the carrier signal, then (12) becomes,

$$VAR\{\hat{\alpha}(r)\} \geq \frac{6}{\left(L(L^2 - 1)SNR\pi^2 cos^2(\alpha)\right)} \quad (13)$$

thus, removing the dependency of carrier frequency from the equation. The standard deviation for different antenna parameters and waveform incident angles in degrees can be obtained using the following equation.

$$stddev = \frac{180}{\pi}\sqrt{VAR\{\hat{\alpha}(r)\}} \quad (14)$$

4.2 Method of Measuring Geometrical Influence on Positioning

The positioning performance is directly influenced by the relative position of the BSs and MT. If the other parameters are similar, depending on the relative distance and orientation of the MT, the positioning performance differs. In this thesis, Position Error Bound (PEB) has been used to visualize the theoretical positioning performance for different reference signals at different geometrical scenarios. The PEB is intricately linked to the CRLB as it is defined to be the square root of position CRLB. If we consider a trilateration with a synchronized clock then [17],

$$PEB = VAR\{\hat{x}\} \geq CRLB = \sqrt{trace\left(\Phi^T(x)\sum^{-1}\Phi(x))^{-1}\right)} \quad (15)$$

Here, Φ(x) is the Jacobian matrix which is obtained by taking partial derivates of the TOA and AOA location measurement model equations with respect to the MT location components x. Additionally, $\sum$ denotes the covariance of the corresponding measurements and trace refers to the sum of the diagonal elements of the matrix.

5. RESULTS AND ANALYSIS

In this chapter, the performance evaluation of 5G uplink and downlink reference signals for positioning has been implemented. In the first section, the resource allocation estimation of the reference signals is realized. After that, the results are discussed in two sections; in the first section TOA and AOA positioning estimation performance have been evaluated with different Signal to Noise Ratio (SNR) values for the reference signals in question, and in the second section geometrical influence of positioning scenario has been delineated for the reference signals.

5.1 Reference Signal Resource Allocation Estimation

In this thesis, DMRS, CSI-RS, and SSB for downlink, and SRS and DMRS for uplink have been considered for positioning performance analysis. PTRS for both uplink and downlink has been omitted due to insignificant frequency domain resource allocation. Given that, 5G will utilize FR1 from 450 MHz to 6 GHz and FR2 mmWave from 24.25 GHz to onwards [6], two different carrier frequencies 3.5 GHz and 30 GHz from FR1 and FR2 respectively have been considered in this analysis. The bandwidth, subcarrier spacing, total number of subcarriers, and the total number of resource blocks for the corresponding carrier frequencies have been described in Table 4 [17].

Table 4 3.5 *GHz and 30 GHz carrier frequency resource allocation*

Carrier Frequency	**Bandwidth**	**Subcarrier Spacing**	**Total Number of Subcarriers**	**Total Number of Resource Blocks**
3.5 GHz	100 MHz	30 kHz	3276	273
30 GHz	400 MHz	120 kHz	3168	264

5G allows quite a lot of flexibility in terms of reference signal resource allocation based on different situations and deployment scenarios. Here, maximum allowable resource allocation has been considered for the reference signal performance analysis. Table 5 illustrates the maximum available resource allocation of the selected reference signals for two carrier frequencies.

Table 5 *Reference signal maximum resource allocation* [61]

Reference Signal	**Transmission Direction**	**Resource Block Structure**	**Maximum Number of Subcarriers per Resource Block**	**Total Number of Subcarriers**	
				3.5 GHz	**30 GHz**
Demodulation Reference Signal	Downlink	Every other subcarrier per resource block	6	1638	1584
Channel State Information Reference Signal	Downlink	Can take up to 32 resource elements	8	2184	2112
Primary and Secondary Synchronization Signal (SS block)	Downlink	240 subcarriers wide and 4 OFDM symbols long	N/A	240	240
Demodulation Reference Signal	Uplink	Up to four symbols per slot and every other subcarrier per resource block	6	1638	1584
Sounding Reference Signal	Uplink	Transmitted in every 2 or 4 subcarriers	6	1638	1584

Since DMRS bandwidth directly relates to PDSCH transmission, different PDSCH allocation is used for DMRS performance estimation.

5.2 TOA Measurement Accuracy for Reference Signals

TOA measurement accuracy is calculated using (11) for both 3.5 GHz and 30 GHz carrier frequencies across the SNR range of -5 to 30 dB for both uplink and downlink reference signals. To cater to different DMRS transmission scenarios three different cases of PDSCH transmission (10%, 50%, and 100% of total bandwidth) have been considered. Therefore, a total number of 163, 819, and 1638 subcarriers are taken for 3.5 GHz and a total number of 158, 792, and 1584 subcarriers are taken for 30 GHz for DMRS TOA accuracy measurement.

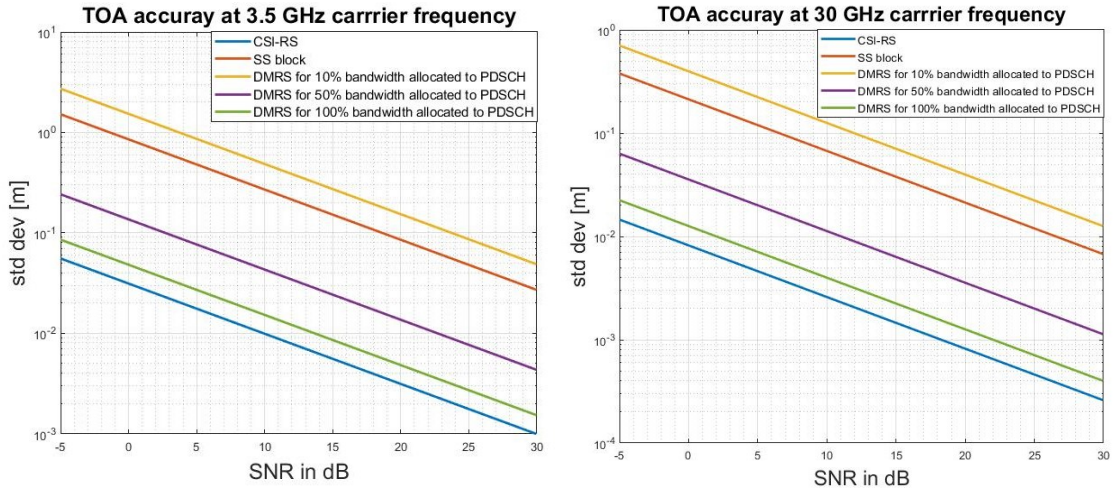

Figure 18 *Theoretical TOA accuracy measurement for downlink reference signals*

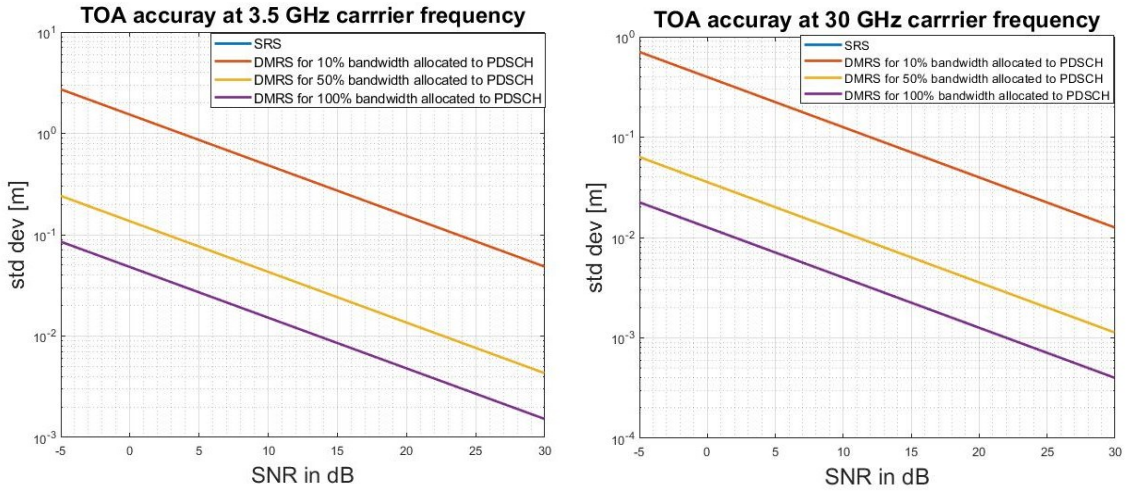

Figure 19 *Theoretical TOA accuracy measurement for uplink reference signals*

As can be seen from Figures 18 and 19, the standard deviations for different reference signals are lower for 30 GHz carrier frequency compared to the 3.5 GHz carrier frequency for both uplink and downlink reference signals despite the fact that the number of subcarriers available is slightly less for 30 GHz carrier frequency as standard deviation

is inversely proportional to the subcarrier spacing and it is higher for 30 GHz carrier frequency. Moreover, the standard deviation decreases with the improvement of SNR value for both cases. Additionally, for downlink, CSI-RS has the lowest standard deviation value followed by DMRS for 100% of total bandwidth. DMRS for 50% of total bandwidth, SSB, and DMRS for 10% of total bandwidth. This is because TOA measurement accuracy directly depends on the frequency domain resource allocation. Since the CSI-RS has the highest number of subcarriers allocated to it and the DMRS with 10% allocated bandwidth has the lowest number of subcarriers allocated to it, CSI-RS has the best performance and DMRS with 10% allocated bandwidth has the worst performance.

For uplink SRS and DMRS for 100% of total bandwidth has the lowest standard deviation followed by DMRS for 50% of total bandwidth and DMRS for 10% of total bandwidth. Therefore, in the uplink, SRS, and DMRS with 100% allocated bandwidth both delivers the most accurate TOA measurement due to larger frequency domain resource allocation compared to the rest. Since DMRS transmission heavily depends on PDSCH bandwidth allocation and it dynamically changes based on demand, for reliable and continuous positioning estimation CSI-RS for downlink and SRS for uplink is the most logical choice for carrying positioning data in addition to the regular channel sounding responsibility. However, for our TOA performance evaluation, we have considered full bandwidth of CSI-RS and SRS to be available for positioning, but in a real scenario, only a portion of the bandwidth will be available which would affect the performance of the positioning accuracy as the variance of the distance estimate is inversely proportional to the number of subcarriers available for positioning as shown in (9). Besides, when there is no data connection available, CSI-RS and SRS reference signals would not be attainable.

5.3 AOA Measurement Accuracy for Reference Signals

AOA measurement accuracy is calculated using (14) for both 3.5 GHz and 30 GHz carrier frequency across the SNR range of -5 to 30 dB. Since the MT orientation is dynamic and unpredictable relative to the BSs during downlink communication, AOA positioning has only been considered for uplink. For 3.5 GHz carrier frequency, three different incident angles 0°, 45°, and 60° and the number of 4 and 8 antenna elements have been

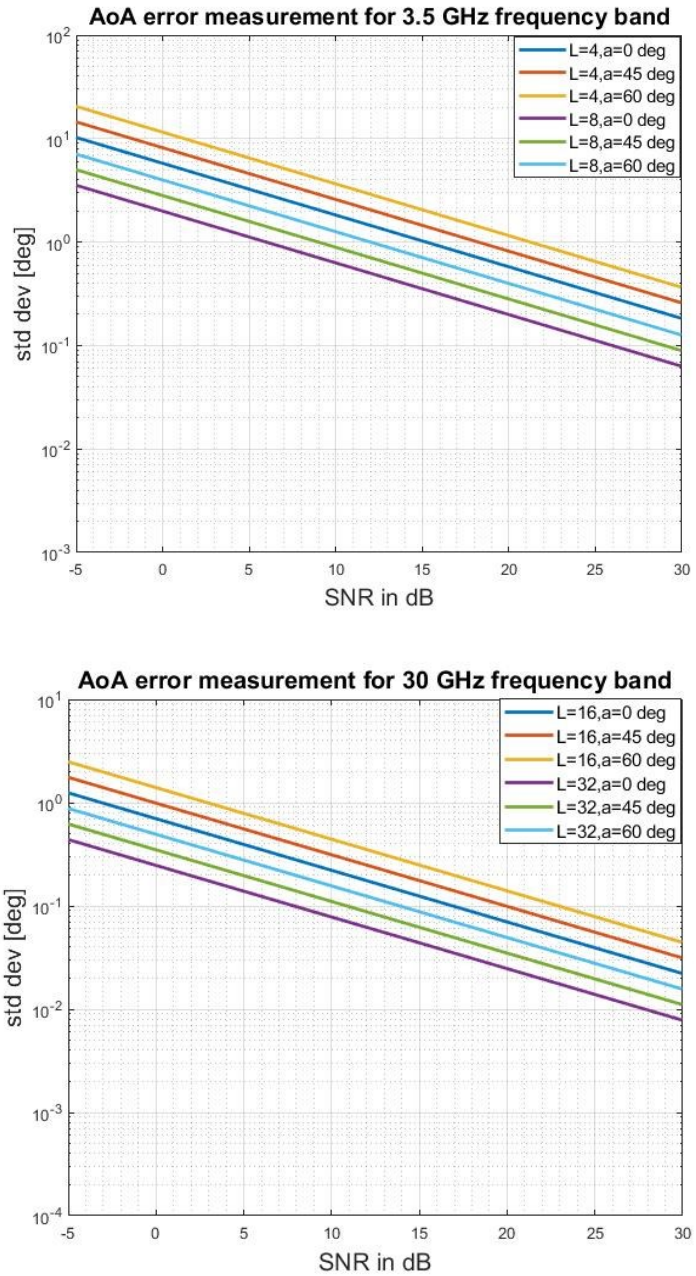

Figure 20 *Theoretical AOA accuracy measurement for uplink reference signals*

considered for AOA performance evaluation. For 30 GHz carrier frequency, three different incident angles 0°, 45°, and 60° and the number of 16 and 32 antenna elements have been considered for AOA performance evaluation.

According to Figure 20, for 3.5 GHz carrier frequency, the lowest standard deviation is achieved when the number of antenna elements is L=8 and the incident angle is a=0. In contrast, the configuration with L=4 and a=60 lead the highest standard deviation value and implying the worst estimation accuracy. For 30 GHz carrier frequency, L=32 and a=0° achieved the lowest standard deviation value implying the best estimation accuracy, and L=16 and a=60° achieved the highest standard deviation value implying the worst estimation accuracy. Comparing between 3.5 GHz and 30 GHz carrier frequency, it can be seen that L=30 and a=0° has the lowest overall standard deviation and thus providing the highest AOA accuracy, proving that AOA positioning accuracy improves with the increase of the number of antenna elements and decrease of the incident angle of the signal as shown in (12).

5.4 Geometrical Influence of Different Positioning Scenarios

Geometrical influence is calculated using (15) for TOA, AOA, and the combination of these two of uplink reference signals for both 3.5 GHz and 30 GHz carrier frequency and geometrical influence of only TOA measurement has been calculated of the downlink reference signals for both carrier frequency. For these evaluations, an area of 400m x 400m and three BSs have been considered. The location and the orientation of the BSs have been kept constant for the measurement of all the reference signals in question. The transmission power and antenna gain have been set to 10 dB, and it is assumed that the MT has an omnidirectional antenna array. The number of antenna elements has been set to 8. The angle between the BS antenna boresight and MT has been measured for each MT location. Also, the communication between the MT and the BSs is considered LOS.

The PEB for TOA based positioning method for downlink reference signals has been considered first. Since geometrical influence across all the downlink reference signals follows similar trends, only CSI-RS and SSB are analyzed to illustrate the difference between higher and lower frequency domain resource allocation. Analyzing Figure 21, it can be seen that overall PEB for CSI-RS is lower at 3.5 GHz carrier frequency compared to that of the 30 GHz carrier frequency. Since the lower the PEB value the higher the positioning accuracy, the CSI-RS at 3.5 GHz carrier frequency performed better than the 30 GHz carrier frequency. This stems from the fact that higher carrier frequencies and bandwidth have significantly higher path loss, and thus attenuates faster and result in a poorer SNR for fixed transmission power and antenna gain. The systems with higher transmission frequency can address poorer SNR performance by increasing the trans-

mission power and antenna gain or by adding more BSs inside the coverage area. Furthermore, it can be seen that the positioning accuracy is greater when the MT is close to the three BSs, and performance degrades gradually as MT moves further from the BSs. It is also interesting to see that the positioning accuracy is much less when the MT is directly behind the BSs antenna direction and other BS are not covering that location even though the MT is much closer to the BS.

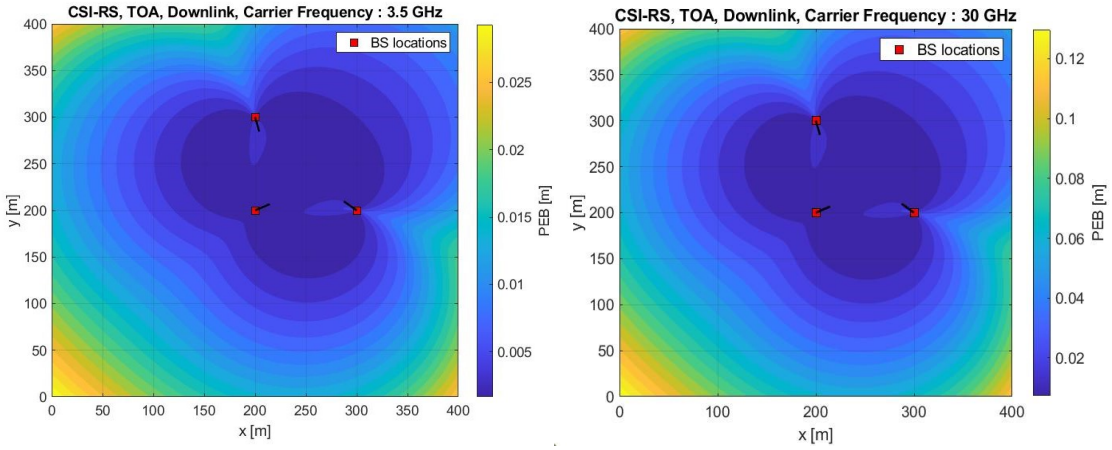

Figure 21 *PEB for TOA positioning for downlink CSI-RS*

For the SS block, it can be seen from Figure 22 that, similar to CSI-RS, the PEB values are lower for the 3.5 GHz carrier frequency compared to the 30 GHz carrier frequency. Therefore, the TOA positioning accuracy for the SS block at 3.5 GHz carrier frequency is better than the 30 GHz carrier frequency.

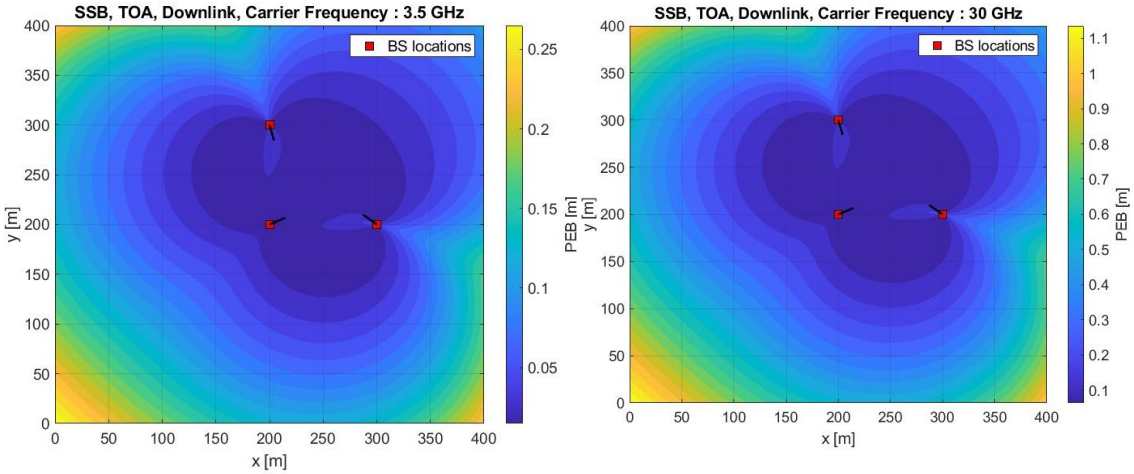

Figure 22 *PEB of TOA positioning method for downlink SS block*

From Figures 21 and 22, it can be seen that PEB values of CSI-RS for 3.5 GHz carrier frequency are the lowest. Thus, CSI-RS performs best in terms of TOA positioning for the different geometrical location of the MT preceded by SS block. It is evident from the observation that, the reference signals with a higher number of subcarriers allocated to

them performed better compared to the reference signals with a lower number of sub-carriers. As for the geometrical influence, the TOA performance degrades as the MT shifts further from the base stations and the strongest positioning estimation has been achieved when the MT is between the three BSs.

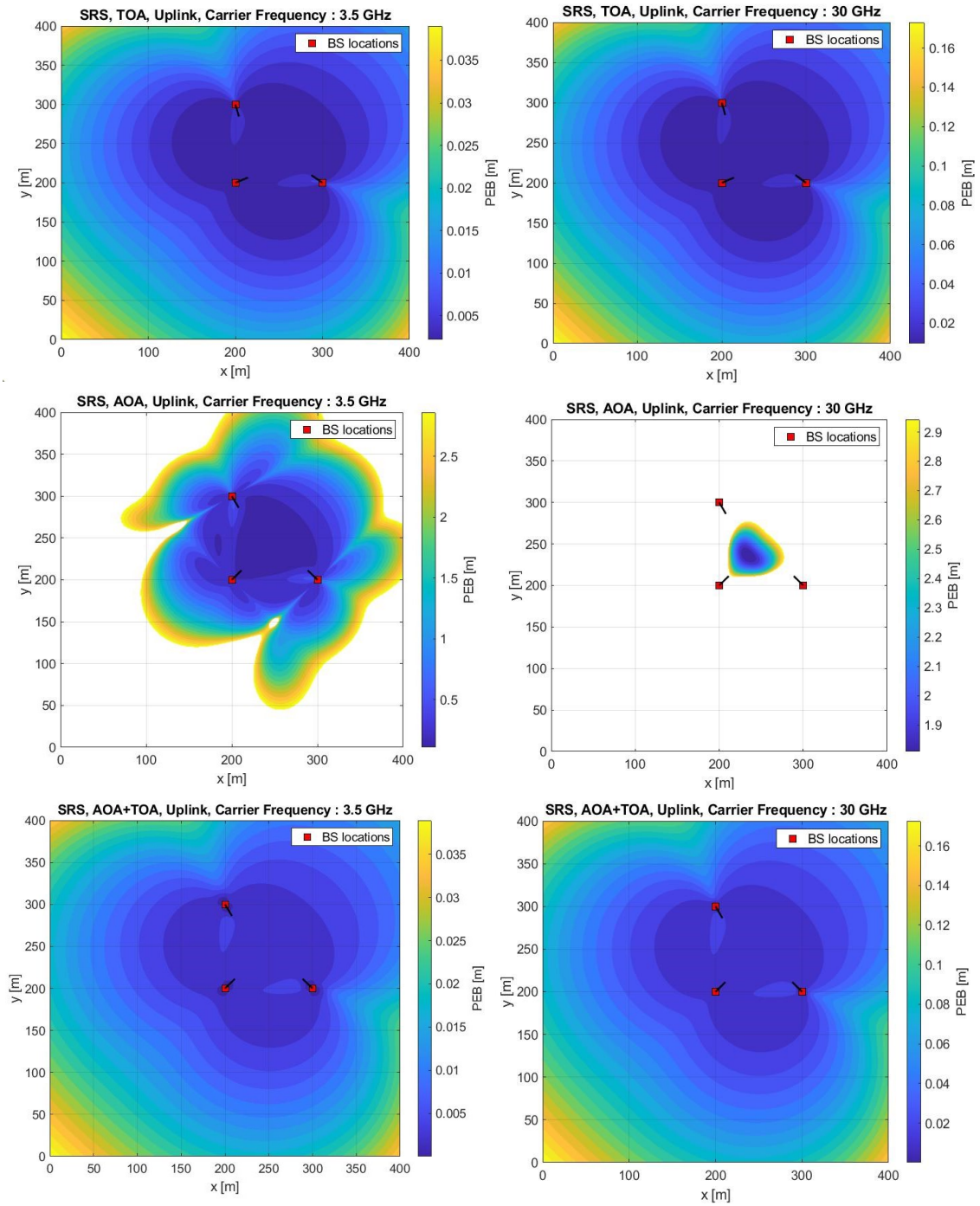

Figure 23 *PEB of TOA, AOA, and TOA+AOA positioning method for uplink SRS*

For the uplink, the geometrical influence on TOA, AOA, and the combination of these two has been evaluated as shown in Figures 23 and 24. Similar to downlink, only SRS

and DMRS with 10% allocated bandwidth are analyzed to illustrate the difference between higher and lower frequency domain resource allocation. The PEB values of SRS for different MT positioning with respect to the three BSs for 3.5 GHz and 30 GHz carrier frequency with TOA, AOA, and TOA plus AOA have been depicted in Figure 23. Akin to downlink reference signals, PEB values of SRS for 3.5 GHz carrier frequency are lower than the 30 GHz carrier frequency for TOA based positioning. This is due to higher carrier frequencies having significantly higher path loss, and thus attenuating faster and resulting in a poorer SNR for fixed transmission power and antenna gain. In terms of AOA, for 3.5 GHz carrier frequency, the three BSs cover most of the measurement area and the PEB values are smaller when the MT is in between the three BSs, and value increases as the MT shifts from the BS. For 30 GHz carrier frequency, the coverage is very limited, and the BSs only cover a tiny fraction of the total measurement area where PEB value is less than 3m in between three BSs and the PEB values are large in the covered portion of the area. Besides, the AOA performance depends on the BS orientations in the uplink. Depending on the orientation of the BSs and the relative location of the MS in the coverage area, the positioning performance varies significantly, which is explained in the later part of this section. It is also evident that the PEB value is larger when the MS is between the Euclidean distance of two BS because MS could be anywhere in the Euclidean distance when that happens. When TOA and AOA positioning methods are combined, similar to TOA, the PEB values are lower at 3.5 GHz carrier frequency compared to 30 GHz carrier frequency. Comparing TOA, AOA, and TOA plus AOA performance, it can be seen that TOA plus AOA provides the lowest PEB values and thus provides the best accuracy for both 3.5 GHz and 30 GHz carrier frequency. Additionally, the combination of TOA and AOA can estimate the MT position with a single BS in two dimensions and thus resulting in lower PEB value around each of the three BSs [39]. The TOA comes in second with slightly inferior performance compared to TOA plus AOA, and finally, AOA, which came third and provided the least positioning accuracy for both carrier frequencies. AOA provided similar coverage to the TOA plus AOA and TOA at 3.5 GHz and smaller coverage to the TOA plus AOA and TOA at 30 GHz carrier frequency.

For DMRS in the uplink, PUSCH allocation of 10% of total bandwidth has been considered. PEB values for two carrier frequencies with TOA, AOA, and TOA plus AOA have been delineated in Figure 24. Analyzing the figures, it can be seen that PEB values for 3.5 GHz carrier frequency are lower than 30 GHz carrier frequency for TOA based positioning. In terms of AOA, both the PEB values are lower and the coverage is better for 3.5 GHz carrier frequency compared to 30 GHz carrier frequency where only a fraction

of the area is covered by the three BSs where PEB value is less than 3m. Finally, for TOA plus AOA, the story is similar to TOA.

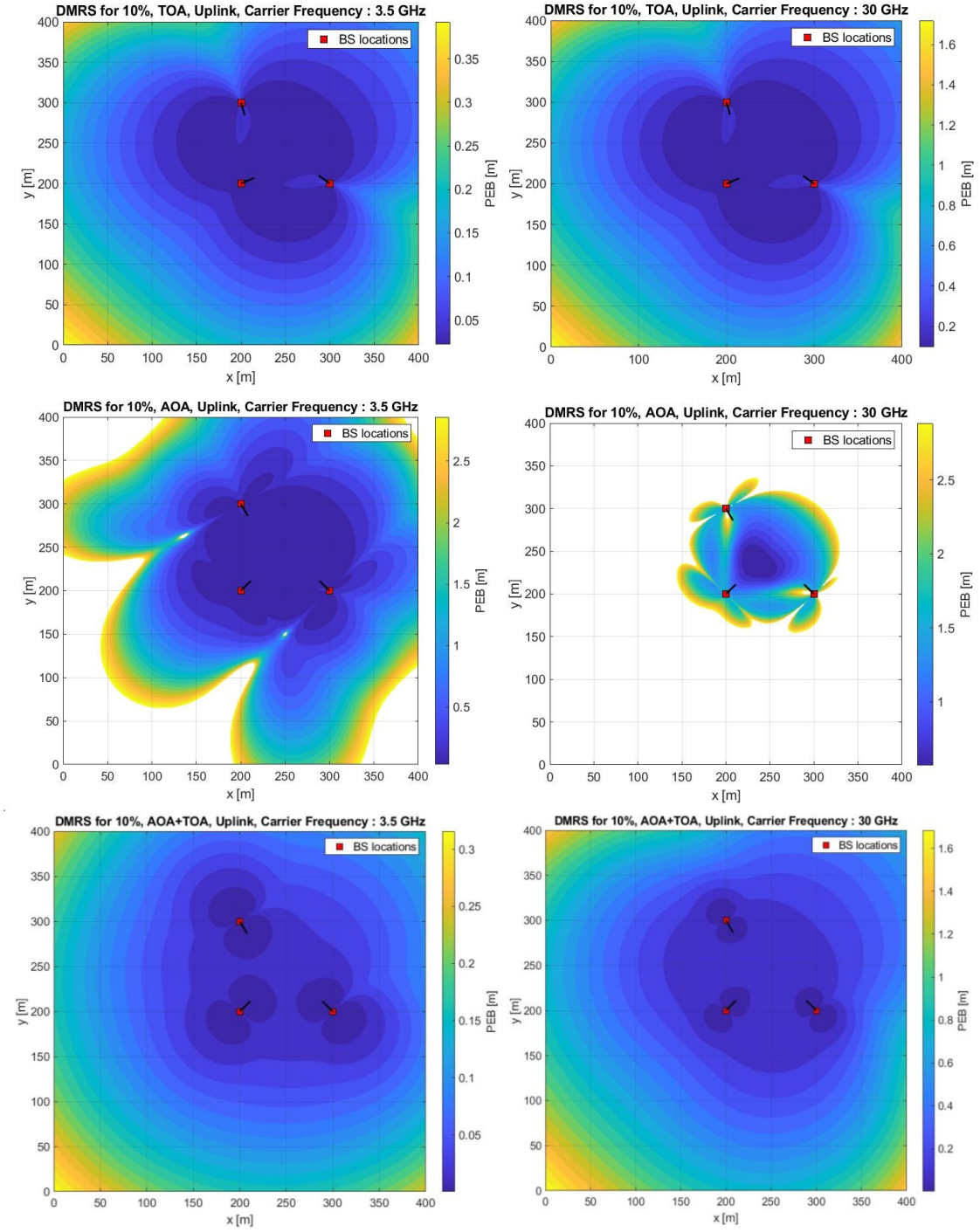

Figure 24 *PEB of TOA, AOA, and TOA+AOA positioning method for 10% uplink DMRS bandwidth allocation*

It is evident that the combination of TOA and AOA has provided lower PEB value across the highest coverage area compared to standalone TOA and AOA. Here it is also clear that the PEB values are lower around each BSs owing to the combination of TOA and AOA having the capability of estimating MT position with a single BS in two dimensions

[15]. TOA comes in second providing a similar coverage range to the TOA plus AOA and only slightly inferior PEB value close to the BSs. Finally. AOA has provided slightly inferior coverage to TOA plus AOA and TOA at 3.5 GHz carrier frequency, but coverage shrank at 30 GHz, and the PEB values are higher for both carrier frequencies compared to TOA plus AOA and TOA. Nonetheless, the performance of AOA can be improved by increasing the number of BSs, sectorising the BSs by adding multiple antennas to cover all directions, and by increasing number of antenna array elements.

Comparing the positioning accuracy for uplink reference signals from Figures 23 and 24, it is clear that the PEB values are lowest for SRS in terms of TOA and combination of TOA and AOA for both 3.5 GHz and 5 GHz carrier frequency. The DMRS for 10% allocated bandwidth comes in next. Similar to downlink, the uplink reference signals with a higher number of subcarriers allocated to them performed better compared to the reference signals with a lower number of subcarriers allocated to them. In terms of AOA positioning accuracy, both reference signals performed very similarly and achieved higher accuracy and coverage at 3.5 GHz carrier frequency compared to 30 GHz due to higher path loss and attenuation and lower SNR value at 30 GHz carrier frequency.

In order to evaluate the performance of AOA with respect to number of antenna array elements, AOA positioning accuracy has been evaluated for two distinct size of antenna arrays, 8 and 16 for DMRS with 10% allocated bandwidth. We have considered 30 GHz carrier frequency for this evaluation. As we can see from Figure 25, the coverage where PEB is less than 3m is considerably better when the number of antenna elements in the antenna arrays for all three BSs have been increased to 16. Apart from coverage, the PEB value is also slightly lower for higher number of antenna array elements.

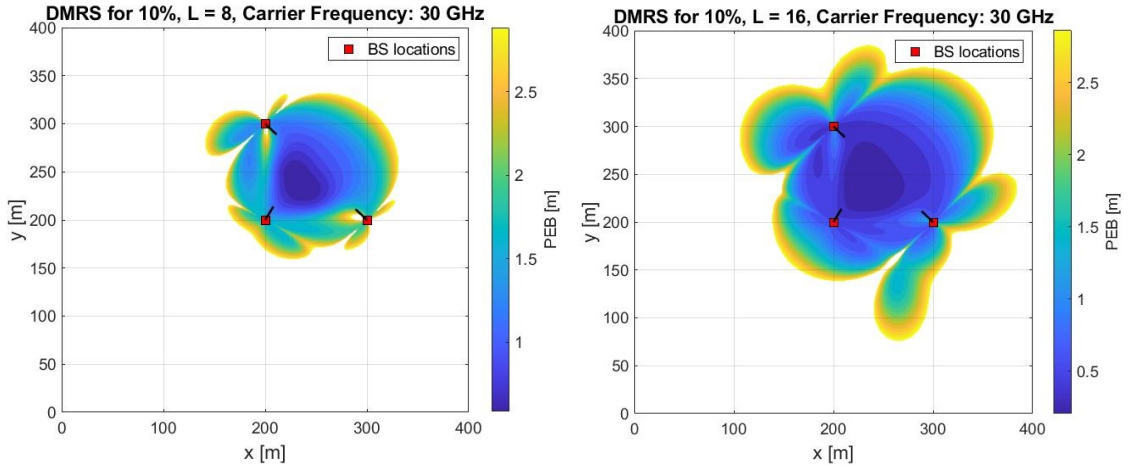

Figure 25 *Theoretical AOA based positioning performance for two different antenna array size*

Next, the impact of additional BSs on AOA positioning performance for our experimental coverage area has been assessed for the same reference signal and carrier frequency as the above scenario. We have increased total number of BSs to five for our assessment and compared it with the previous three BS setup . As can be seen from Figure 26, the addition of two BSs in our experimental area has increased the coverage of AOA based positioning considerably. The PEB value is also slightly lower in case of five BSs signifying increased AOA positioning performance.

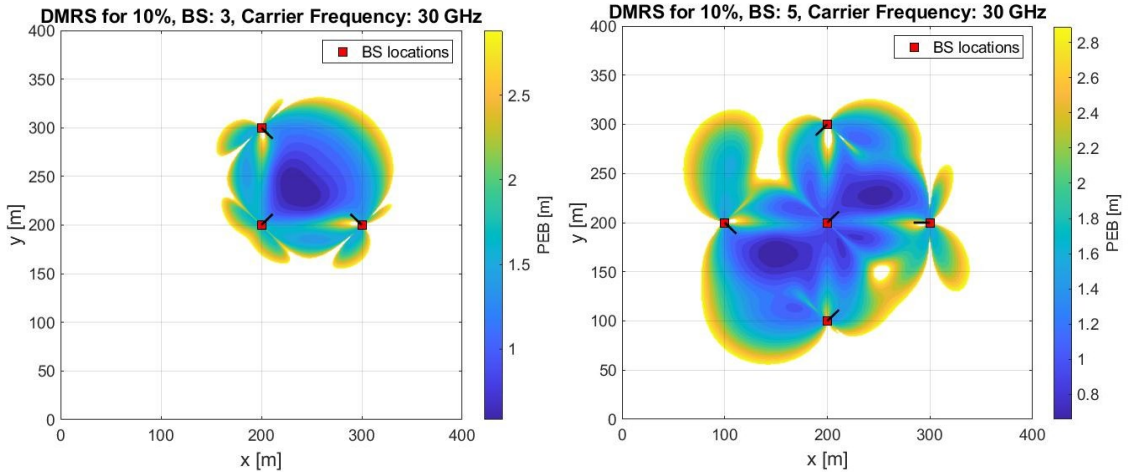

Figure 26 *Effect of additional BSs on theoretical AOA based positioning performance*

Finally, the effect of multiple antennas under each BS on AOA positioning performance has been evaluated. For this scenario, we have divided each BS into three cells by adding three antennas placed 120 degrees apart to cover the whole 360 degrees. Then, we have compared the AOA performance for sectorized BSs with our previous single antenna setup. We have considered the same reference signal and carrier frequency as the above scenario. Depending on the location of the MT in our experimental area, we have calculated the angles between MT and all BSs, and determined the serving cells to be cells whose boresight direction is closest to the MT-BS direction.

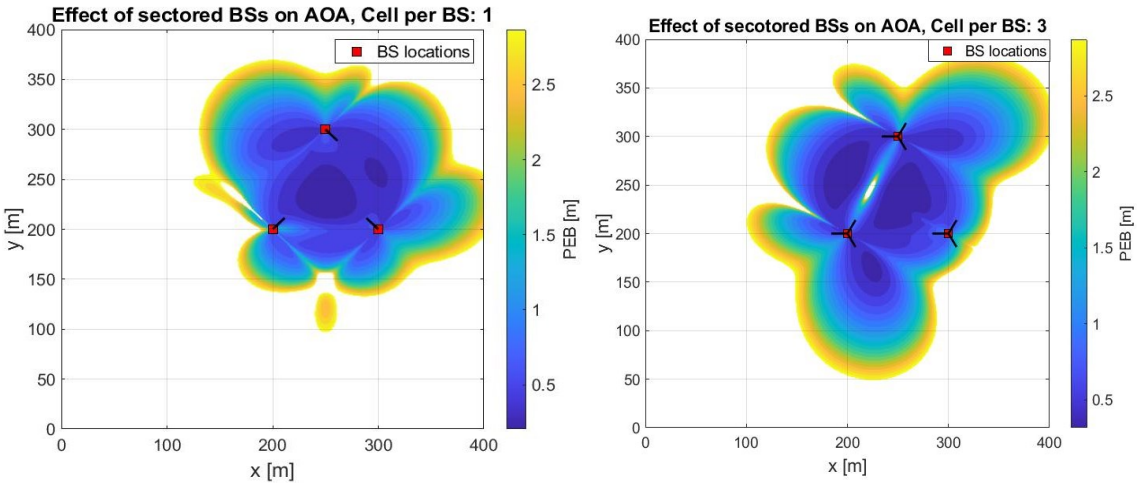

Figure 27 *Effect of sectored BSs on theoretical AOA based positioning performance*

As illustrated in Figure 27, it is evident that the sectorization of the BSs have increased the coverage where PEB is less than 3m. The PEB value within this coverage area is also marginally better compared to the single antenna setup. However, depending on the position and antenna orientation of the BSs, the performance difference could be increased or decreased for AOA based positioning.

As discussed before, 5G will introduce mmWave frequency bands (24 GHz to 100 GHz and above). Due to the higher associated path loss of those frequencies, 5G aims to deploy denser BS configuration compared to previous technologies. Moreover, higher carrier frequencies will also allow implementing higher number of antenna elements within each antenna. Thus, 5G paves the way for higher AOA based positioning performance due to the increased number of antenna arrays and BSs compared to the previous technologies.

5.4.1 Effect of Geometry on Positioning Performance

In order to evaluate the effect of base station location and antenna orientation on the positioning performance, PEB for SRS in uplink direction for 3.5 GHz carrier frequency has been considered. Two separate sets of BS locations and for each set of locations two different BS antenna orientations have been considered for the first two scenarios. In the third scenario, all three BSs have been placed on single line formation to emulate real life highway or rail line BS placement. The positioning techniques considered are AOA and TOA. The combination of TOA and AOA has been excluded due to similar positioning performance compared to TOA.

Firstly, the effect of geometry on theoretical AOA based positioning has been observed. Three different scenarios of BS locations and two different sets of BS antenna boresight angles for first two scenarios have been illustrated in Figure 28. In scenario 1, the distances between 3 BSs are large. If we compare the AOA accuracy between these two sets of angles, we can see that the coverage varies significantly. For the first case, only a fraction of the area has been covered by AOA (PEB < 3m), but for the second case, the majority of the area has been covered. In scenario 2, the distances between the three BSs are relatively small and the placement of the BSs is also different compared to scenario 1. Comparing the two cases of BS antenna boresight angle for scenario 2, we can see that the coverage is comparable between the two cases, but the coverage area has been shifted due to the change in the BS antenna boresight angle. Comparing between two scenarios, it can be seen that the PEB values are smaller for scenario 2, which signifies higher positioning accuracy when BSs are closer to each other.

The scenario 3 has been designed to mimic the highway or rail line BS configuration. Here, in the first case we can see that AOA positioning accuracy along the straight line between BSs is almost non existent as it is not possible to determine the MT location with AOA principle when MT is along the Euclidian distance between the BSs. In order to mitigate this effect, BS placement in a zigzag like pattern could be implemented. In the second case of the scenario 3, we can see that the zigzag like placement of BSs have improved the positioning performance along the straight line between the BSs.

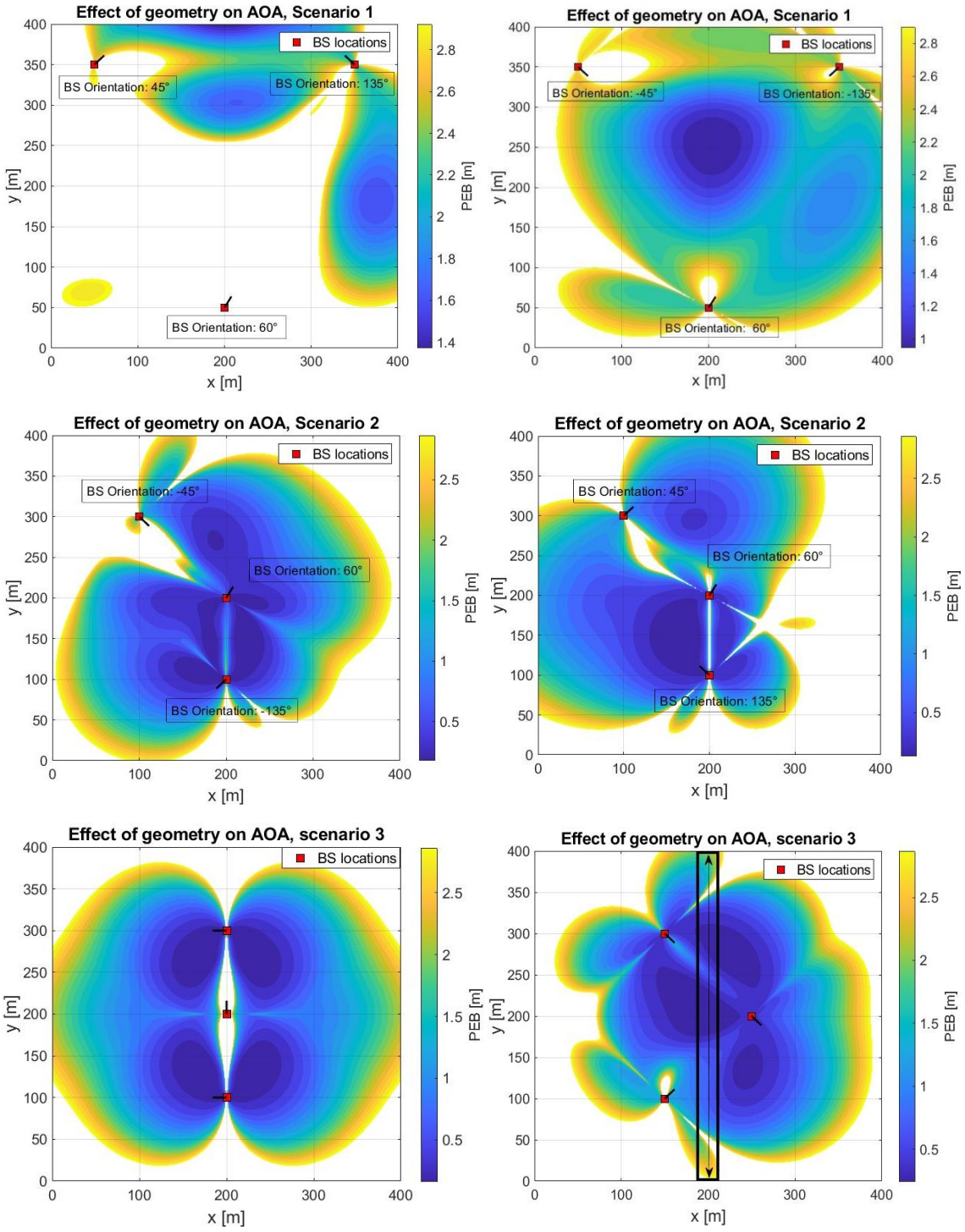

Figure 28 *Effect of geometry on theoretical AOA positioning accuracy*

Next, the effect of geometry on theoretical TOA based positioning has been evaluated as can be seen from Figure 29. Similar to AOA, two different scenarios of BS locations and two different cases of BS antenna boresight angles for each scenario for TOA have been illustrated. In scenario 1, the distances between BSs are higher compared to scenario 2. If we compare TOA accuracy for two different sets of BS antenna boresight angles for both scenarios, we can see that there is no effect of BS antenna orientation on TOA accuracy. However, comparing the two scenarios, it is apparent that within our coverage area, the PEB values are smaller in the majority of the coverage area in scenario 2 compared to scenario 1, signifying higher TOA accuracy when BSs are closer together. The scenario 3 has not been implemented for TOA based positioning due to no effect of BS antenna orientation on TOA accuracy.

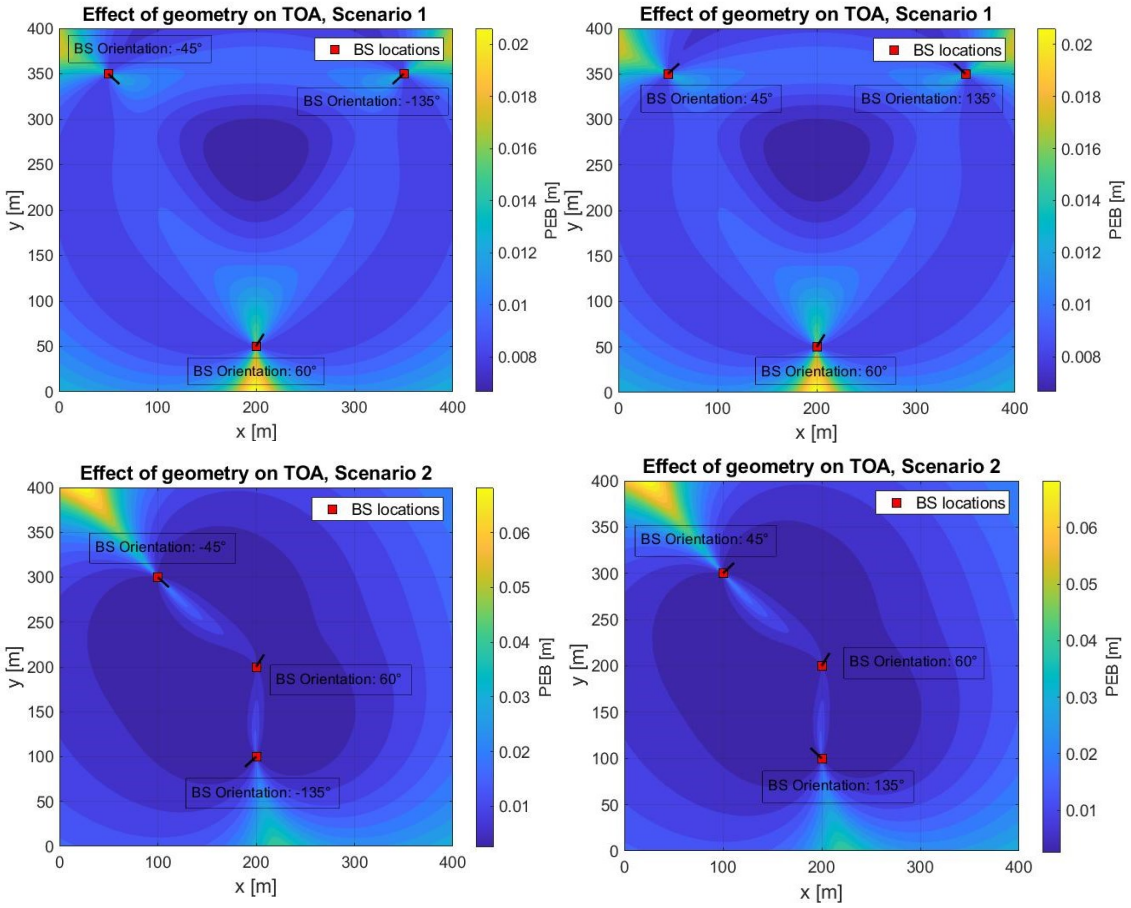

Figure 29 *Effect of geometry on theoretical TOA positioning accuracy*

Based on the above evaluations, it can be rationalized that the effect of BS antenna boresight angle will be minimal for the combination of theoretical TOA and AOA based positioning as the TOA accuracy significantly outperforms the AOA accuracy in our experimental scenario. Also, the positioning accuracy will also be similar for different locations of the BSs within our experimental coverage area.

5.5 Comparison with 5G Positioning Requirements

The PEB value depends on a number of factors and based on different carrier frequencies and resource allocation scenarios, different PEB values are achieved for different uplink and downlink reference signals as delineated in Figures 21-24. These PEB values range from 0.005 m to 2.9 m at different distances from the 3 BS. 3GPP has specified positioning accuracy requirements at different positioning service levels which are described in section 2.4. The achievable horizontal positioning accuracy and service levels for uplink and downlink reference signals at different carrier frequencies are depicted in Tables 6 – 9.

Table 6 *Theoretical TOA downlink performance* comparison with 5G positioning requirements

Reference Signal	**Transmission Direction**	**Theoretical Achieved Accuracy (m)**		**Coverage (m)**	**Maximum achievable Positioning Service Level**	
		3.5 GHz	**30 GHz**		**3.5 GHz**	**30 GHz**
CSI-RS	Downlink	0.005-0.025	0.02-0.12	400x400	7	7
SS block	Downlink	0.05-0.25	0.10-1.10	400x400	7-6	7-5

Table 7 *Theoretical TOA uplink performance* comparison with 5G positioning requirements

Reference Signal	**Transmission Direction**	**Theoretical Achieved Accuracy (m)**		**Coverage (m)**	**Maximum achievable Positioning Service Level**	
		3.5 GHz	**30 GHz**		**3.5 GHz**	**30 GHz**
SRS	Uplink	0.005-0.03	0.02-0.16	400x400	7	7
DMRS with 10% BW	Uplink	0.05-0.35	0.20-1.60	400x400	7-6	7-6

Table 8 *Theoretical AOA uplink performance* comparison with 5G positioning requirements

Reference Signal	**Transmission Direction**	**Theoretical Achieved Accuracy (m)**		**Coverage (m)**	**Maximum achievable Positioning Service Level**	
		3.5 GHz	**30 GHz**		**3.5 GHz**	**30 GHz**
SRS	Uplink	0.5-2.5	1.9-2.9	~200x200	6-2	6-2
DMRS with 10% BW	Uplink	0.5-2.5	1.0-2.5	~300x300	6-2	6-2

Table 9 *Theoretical TOA + AOA uplink performance* comparison with 5G positioning requirements

Reference Signal	**Transmission Direction**	**Theoretical Achieved Accuracy (m)**		**Coverage (m)**	**Maximum achievable Positioning Service Level**	
		3.5 GHz	**30 GHz**		**3.5 GHz**	**30 GHz**
SRS	Uplink	0.005-0.035	0.02-0.16	400x400	7	7
DMRS with 10% BW	Uplink	0.05-0.3	0.2-1.6	400x400	7-6	7-6

The theoretical TOA positioning accuracies achieved for downlink CSI-RS for both carrier frequencies are capable of positioning service level 7 across the whole coverage area of our experimental system of 400m x 400m. The accuracy achieved for downlink SS block for 3.5 GHz carrier frequency is capable of positioning service levels from 7 to 6 and for 30 GHz carrier frequency from 7 to 5 based on the distance between BSs and MT.

The theoretical TOA positioning accuracies achieved for uplink SRS for both carrier frequencies are capable of positioning service level 7 across the whole coverage area. The accuracy achieved for uplink DMRS with 10% allocated bandwidth for both carrier frequencies varies between 7 to 6 achievable service levels based on the distance between BSs and MT. The theoretical AOA positioning accuracy achieved for uplink SRS for both carrier frequencies is capable of positioning service levels from 6 to 2 based on the distance between the BSs and MT within the approximately 200m x 200m area covered.

The accuracy achieved for uplink DMRS with 10% allocated bandwidth for 3.5 GHz carrier frequency varies between 7 to 6 achievable service levels and for 30 GHz carrier frequency from 6 to 2 achievable service levels based on the distance between the BSs and MT within the approximately 300m x 300m area covered. The theoretical TOA + AOA positioning accuracies achieved for uplink SRS for both carrier frequencies are capable of positioning service level 7 across the whole coverage area. Finally, the accuracies achieved for uplink DMRS with 10% allocated bandwidth for 3.5 GHz carrier frequency are capable of positioning service level 7 across the whole coverage area and for 30 GHz capable of positioning service level from 7 to 6 based on the distance between the BSs and the MT. Thus, 5G high accuracy positioning is achievable utilizing existing reference signals even without introducing a dedicated positioning reference signal. Moreover, depending on the scenario, different reference signals could be utilized to determine the MT location. For example, where precise positioning accuracy is not required or where there is no data connection available, SSB could be used to determine the MT position. Similarly, where accurate positioning is strict priority, DMRS or SRS, or combination of multiple reference signals and positioning techniques could be utilized to determine the MT position.

5.6 Time Domain Resource Allocation

Besides the frequency domain, the time domain resource allocation also has a crucial impact on positioning and navigation applications. Self-driving cars, indoor positioning, UAV, and many other applications require precise and real-time positioning [15]. Reference signals with higher time domain resource allocation and repetition rate will provide more smooth navigation and real-time and accurate positioning. 5G allows flexible time domain resource allocation based on different usage scenarios for the reference signals [6]. Depending on different positioning requirements, time-domain resource allocation and the repetition rate of the reference signals could be adjusted.

6. CONCLUSION

The new 5G mobile radio standard aims to provide a broad range of services in the area of industry 4.0, IoT, smart city, autonomous vehicles, healthcare, emergency services, different location aware services, etc. To meet these requirements, providing high accuracy positioning is crucial. Since GNSS based positioning does not provide the expected level of accuracy especially in the indoor environment, and thanks to the introduction of many advanced new features and technologies, 5G network based positioning aims to offer precise positioning solution for both indoor and outdoor environments to cater to the emerging and upcoming positioning requirements.

In this thesis, we have provided a detailed introduction of 5G NR, its scope, new uses cases, and improvements over previous mobile network technology standards. We have investigated the use cases for 5G based positioning and what improvements it will bring to the table. Furthermore, we have described the working principle of different existing positioning technologies, in particular, GNSS based and wireless communication based positioning technologies. We have also examined the 3GPP positioning requirements in 5G for different deployment scenarios and use cases.

Afterward, we have analyzed 5G uplink and downlink reference signals, their frame structure, and time domain and frequency domain resource allocation. We have compared resource allocation and repetition rates between these reference signals and figured out their maximum allowable resource allocation. Based on the finding, we have decided which reference signals are suitable to be used for positioning purposes. We have also illustrated the variable 5G NR frame structure for different subcarrier spacing at different carrier frequencies and bandwidth at this phase. In addition, we have evaluated and described the theory of TOA and AOA positioning performance estimation methodology.

Next, we have compared TOA measurement accuracy for uplink and downlink reference signals across different SNR range for two different carrier frequencies. Based on the conducted numerical evaluations, CSI-RS for downlink and, SRS and DMRS for 100% bandwidth allocated for PUSCH transmission for uplink performed the best. We have also measured AOA accuracy for different numbers of antenna elements and incident angles of the signal and observed that AOA positioning accuracy increases with the increase of the number of antenna elements and the decrease of the incident angle of the signal. Additionally, we have measured the geometrical influence of reference signals for

TOA and AOA across a predefined area covered by three base stations. In the downlink, CSI-RS provided the highest accuracy over the whole coverage area in terms of TOA accuracy measurement. In the uplink, SRS provided the highest accuracy across the whole coverage area in terms of TOA and TOA plus AOA accuracy measurement. All the uplink reference signals performed similarly in terms of AOA accuracy measurement. We have also examined the effect of number of antenna array elements, denser BS configuration, and sectored BS on AOA positioning performance and discussed how these inherent 5G NR features will pave the way for higher AOA based positioning accuracy compared to previous technologies. Moreover, we have evaluated the effect of geometry (BS location and antenna orientation) on AOA and TOA based positioning methods and deduced that the AOA accuracy and coverage is heavily influenced by the geometry but the effect of geometry on TOA is insignificant. Finally, we have compared our achieved positioning accuracy with 5G positioning requirements and concluded that utilizing existing reference signals for high-accuracy positioning is a viable alternative to introducing a new dedicated reference signal for positioning, and based on different positioning scenarios, different standalone reference signals or combination of reference signals and positioning techniques could be utilized.

5G network based positioning is coming and lots of research are now ongoing to deliver the promised accuracy and performance when it is deployed. In our research, we have provided an alternative solution of utilizing the already existing or defined reference signals for positioning solution instead of creating a dedicated positioning reference signal for 5G.

REFERENCES

[1] GPS.gov: GPS Accuracy, https://www.gps.gov/systems/gps/performance/accuracy/ (accessed February 15, 2020).

[2] 3GPP TR 38.855. Study on NR positioning support (Release 16).

[3] *5G Vision. The 5G Infrastructure Public Private Partnership: the next generation of communication networks and services.*, https://5g-ppp.eu/wp-content/uploads/2015/02/5G-Vision-Brochure-v1.pdf (accessed February 15, 2020).

[4] Lohan ES, Koivisto M, Galinina O, et al. Benefits of Positioning-Aided Communication Technology in High-Frequency Industrial IoT. *IEEE Communications Magazine* 2018; 56: 142–148.

[5] 3GPP TS 38.211. Physical channels and modulation (Release 15).

[6] Dahlman E, Parkvall S, Sköld J. *5G NR: The Next generation wireless Access technology*. Elsevier, 2018. Epub ahead of print August 17, 2018. DOI: 10.1016/C20170013472.

[7] *Making 5G NR a reality Leading the technology inventions for a unifi ed, more capable 5G air interface*, https://www.qualcomm.com/media/documents/files/whitepaper-making-5g-nr-a-reality.pdf (2016, accessed May 6, 2020).

[8] What is enhanced Mobile Broadband (eMBB), https://5g.co.uk/guides/what-is-enhanced-mobile-broadband-embb/ (accessed May 7, 2020).

[9] Davidović M, Tomić I, Drajić D, et al. On the impact of NB-IoT on LTE MBB downlink performance. *Telfor Journal* 2019; 11: 20–24.

[10] 5G Americas White Paper Explores 5G Services, Use Cases, and Market Implications - Technology@Intel, https://blogs.intel.com/technology/2017/12/5g-americas-white-paper-explores-5g-services-use-cases-and-market-implications/#gs.weg7ll (accessed February 15, 2020).

[11] Popovski P, Stefanović Č, Nielsen JJ, et al. Wireless access in Ultra-Reliable Low-Latency Communication (URLLC). *arXiv*. Epub ahead of print October 16, 2018. DOI: 10.1109/tcomm.2019.2914652.

[12] 3GPP TS 21.916. Release description; Release 16, https://www.3gpp.org/DynaReport/21916.htm (accessed April 12, 2020).

[13] 3GPP TS 21.917. Release description: Release 17, https://www.3gpp.org/release-17.

[14] Talvitie J, Koivisto M, Levanen T, et al. Radio positioning and tracking of high-speed devices in 5G NR networks: System concept and performance. In:

European Signal Processing Conference. European Signal Processing Conference, EUSIPCO, 2019. Epub ahead of print September 1, 2019. DOI: 10.23919/EUSIPCO.2019.8902731.

[15] Wymeersch H, Seco-Granados G, Destino G, et al. 5G mmwave positioning for vehicular networks. *IEEE Wireless Communications* 2017; 24: 80–86.

[16] Chaloupka Z. Technology and standardization gaps for high accuracy positioning in 5g. *IEEE Communications Standards Magazine* 2017; 1: 59–65.

[17] Sand Stephan, Dammann Armin, Mensing Christian. *Positioning in wireless communications systems*. Wiley, 2014.

[18] Wait JR. The Ancient and Modern History of EM Ground-Wave Propagation. *IEEE Antennas and Propagation Magazine* 1998; 40: 7–24.

[19] Zhou L, Xi X, Liu J, et al. LF ground-wave propagation over irregular terrain. *IEEE Transactions on Antennas and Propagation* 2011; 59: 1254–1260.

[20] Engel U. A geolocation method using TOA and FOA measurements. In: *Proceedings - 6th Workshop on Positioning, Navigation and Communication, WPNC 2009*. 2009, pp. 77–82.

[21] Brown A, Sturza M. The Effect of Geometry on Integrity Monitoring Performance. 1990; 121–129.

[22] GPS for Land Surveyors - 4th Edition - Jan Van Sickle - Routledge Boo, https://www.routledge.com/GPS-for-Land-Surveyors/Sickle/p/book/9781466583108 (accessed September 12, 2020).

[23] Drane C, Macnaughtan M, Scott C. Positioning GSM telephones. *IEEE Communications Magazine* 1998; 36: 46–59.

[24] Tahat A, Kaddoum G, Yousefi S, et al. A Look at the Recent Wireless Positioning Techniques with a Focus on Algorithms for Moving Receivers. *IEEE Access* 2016; 4: 6652–6680.

[25] Güvenç I, Chong CC. A survey on TOA based wireless localization and NLOS mitigation techniques. *IEEE Communications Surveys and Tutorials* 2009; 11: 107–124.

[26] Yang G, Zhao L, Dai Y, et al. A KFL-TOA UWB indoor positioning method for complex environment. In: *Proceedings - 2017 Chinese Automation Congress, CAC 2017*. Institute of Electrical and Electronics Engineers Inc., 2017, pp. 3010–3014.

[27] Cong L, Zhuang W. Non-line-of-sight error mitigation in TDOA mobile location. In: *Conference Record / IEEE Global Telecommunications Conference*. 2001, pp. 680–684.

[28] A Look at the Recent Wireless Positioning Techniques With a Focus on Algorithms for Moving Receivers, https://www.researchgate.net/publication/309846689_A_Look_at_the_Recent_Wireless_Positioning_Techniques_With_a_Focus_on_Algorithms_for_Moving_Receivers (accessed September 12, 2020).

[29] Bocquet M, Loyez C, Benlarbi-Delaï A. Using enhanced-TDOA measurement for indoor positioning. *IEEE Microwave and Wireless Components Letters* 2005; 15: 612–614.

[30] Catovic A, Sahinoglu Z. The Cramer-Rao bounds of hybrid TOA/RSS and TDOA/RSS location estimation schemes. *IEEE Communications Letters* 2004; 8: 626–628.

[31] Li C, Weihua Z. Hybrid TDOA/AOA mobile user location for wideband CDMA cellular systems. *IEEE Transactions on Wireless Communications* 2002; 1: 439–447.

[32] Fokin G. AOA measurement processing for positioning using unmanned aerial vehicles. In: *2019 IEEE International Black Sea Conference on Communications and Networking, BlackSeaCom 2019*. Institute of Electrical and Electronics Engineers Inc., 2019. Epub ahead of print June 1, 2019. DOI: 10.1109/BlackSeaCom.2019.8812834.

[33] Deligiannis N, Louvros S. Hybrid TOA-AOA location positioning techniques in GSM networks. *Wireless Personal Communications* 2010; 54: 321–348.

[34] Trevisani E, Vitaletti A. Cell-ID location technique, limits and benefits: An experimental study. In: *Proceedings - IEEE Workshop on Mobile Computing Systems and Applications, WMCSA*. 2004, pp. 51–60.

[35] Venkatraman S, Caffery J. Hybrid TOA/AOA techniques for mobile location in non-line-of-sight environments. In: *2004 IEEE Wireless Communications and Networking Conference, WCNC 2004*. Institute of Electrical and Electronics Engineers Inc., 2004, pp. 274–278.

[36] Trevisani E, Vitaletti A. Cell-ID location technique, limits and benefits: An experimental study. In: *Proceedings - IEEE Workshop on Mobile Computing Systems and Applications, WMCSA*. 2004, pp. 51–60.

[37] Wigren T. Adaptive enhanced cell-ID fingerprinting localization by clustering of precise position measurements. *IEEE Transactions on Vehicular Technology* 2007; 56: 3199–3209.

[38] Ficco M, Russo S. A hybrid positioning system for technology-independent location-aware computing. *Software: Practice and Experience* 2009; 39: 1095–1125.

[39] Ahmed EJ, Suliman S-MMA. Locating GSM Subscribers Using Hybrid Cell-ID and Time Advance (TA) Positioning, http://repository.sustech.edu//handle/123456789/6725 (2009, accessed November 18, 2020).

[40] Mazuelas S, Lago FA, González D, et al. Dynamic estimation of optimum path loss model in a RSS positioning system. In: *Record - IEEE PLANS, Position Location and Navigation Symposium*. 2008, pp. 679–684.

[41] Zhou Y, Law CL, Xia J. Ultra low-power UWB-RFID system for precise location-aware applications. In: *2012 IEEE Wireless Communications and Networking Conference Workshops, WCNCW 2012*. 2012, pp. 154–158.

[42] Mazuelas S, Lago FA, González D, et al. Dynamic estimation of optimum path loss model in a RSS positioning system. In: *Record - IEEE PLANS, Position Location and Navigation Symposium*. 2008, pp. 679–684.

[43] Tiemann J, Schweikowski F, Wietfeld C. Design of an UWB indoor-positioning system for UAV navigation in GNSS-denied environments. In: *2015 International Conference on Indoor Positioning and Indoor Navigation, IPIN 2015*. Institute of Electrical and Electronics Engineers Inc., 2015. Epub ahead of print December 3, 2015. DOI: 10.1109/IPIN.2015.7346960.

[44] Alarifi A, Al-Salman A, Alsaleh M, et al. Ultra Wideband Indoor Positioning Technologies: Analysis and Recent Advances. *Sensors* 2016; 16: 707.

[45] Use Cases | Monitoring and Asset Tracking in the Healthcare Sector, https://www.infsoft.com/use-cases/monitoring-and-asset-tracking-in-the-healthcare-sector (accessed October 8, 2020).

[46] 3GPP TS 22.261. Service requirements for the 5G system.

[47] Want R. An introduction to RFID technology. *IEEE Pervasive Computing* 2006; 5: 25–33.

[48] Bai YB, Wu S, Wu H, et al. *Overview of RFID-Based Indoor Positioning Technology*.

[49] Keating R, Saily M, Hulkkonen J, et al. Overview of positioning in 5G new radio. In: *Proceedings of the International Symposium on Wireless Communication Systems*. VDE Verlag GmbH, 2019, pp. 320–324.

[50] Ali A. Zaidi RBMASFVM-CZW. Designing for the future: the 5G NR physical layer - Ericsson, https://www.ericsson.com/en/reports-and-papers/ericsson-technology-review/articles/designing-for-the-future-the-5g-nr-physical-layer (accessed September 13, 2020).

[51] Lien SY, Shieh SL, Huang Y, et al. 5G New Radio: Waveform, Frame Structure, Multiple Access, and Initial Access. *IEEE Communications Magazine* 2017; 55: 64–71.

[52] Noh G, Hui B, Kim J, et al. DMRS design and evaluation for 3GPP 5G new radio in a high speed train scenario. In: *2017 IEEE Global Communications Conference, GLOBECOM 2017 - Proceedings*. Institute of Electrical and Electronics Engineers Inc., 2017, pp. 1–6.

[53] Dahlman E, Parkvall S, Sköld J. Channel-State Information and Full-Dimension MIMO. In: *4g, LTE Evolution and the Road to 5G*. Elsevier, 2016, pp. 269–283.

[54] Lin Z, Li J, Zheng Y, et al. SS/PBCH Block Design in 5G New Radio (NR). In: *2018 IEEE Globecom Workshops, GC Wkshps 2018 - Proceedings*. Institute of Electrical and Electronics Engineers Inc., 2019. Epub ahead of print February 19, 2019. DOI: 10.1109/GLOCOMW.2018.8644466.

[55] Qi Y, Hunukumbure M, Nam H, et al. On the Phase Tracking Reference Signal (PT-RS) Design for 5G New Radio (NR). In: *IEEE Vehicular Technology Conference*. Institute of Electrical and Electronics Engineers Inc., 2018. Epub ahead of print July 2, 2018. DOI: 10.1109/VTCFall.2018.8690852.

[56] Dahlman E, Parkvall S, Sköld J. *5G NR: The Next generation wireless Access technology*. Elsevier, 2018. Epub ahead of print August 17, 2018. DOI: 10.1016/C20170013472.

[57] 5G NR Uplink Carrier Waveform Generation - MATLAB & Simulink, https://www.mathworks.com/help/5g/gs/uplink-carrier-waveform-generation.html (accessed September 13, 2020).

[58] TSGR. *TS 138 211 - V15.2.0 - 5G; NR; Physical channels and modulation (3GPP TS 38.211 version 15.2.0 Release 15)*, https://portal.etsi.org/TB/ETSIDeliverableStatus.aspx (2018, accessed May 31, 2020).

[59] 3GPP TS 38.101. NR; User Equipment (UE) radio transmission and reception.

[60] Qualcomm. *Global update on spectrum for 4G & 5G*, https://www.qualcomm.com/media/documents/files/spectrum-for-4g-and-5g.pdf (2018, accessed November 18, 2020).

[61] Tsung-Yu Chen, Chien-Ching Chiu, Ting-Chieh Tu. Mixing and combining with AOA and TOA for the enhanced accuracy of mobile location. Institution of Engineering and Technology (IET), 2005, pp. 276–280.